2015

PH RESPONSIVE, ADHESIVE HYDROGELS BASED ON REVERSIBLE CATECHOL - BORONIC ACID COMPLEXATION

Ameya Ravindra Narkar
Michigan Technological University

PH RESPONSIVE, ADHESIVE HYDROGELS BASED ON REVERSIBLE CATECHOL - BORONIC ACID COMPLEXATION

By

Ameya Ravindra Narkar

A THESIS

Submitted in partial fulfillment of the requirements for the degree of

MASTER OF SCIENCE

In Biomedical Engineering

MICHIGAN TECHNOLOGICAL UNIVERSITY

2015

This thesis has been approved in partial fulfillment of the requirements for the Degree of MASTER OF SCIENCE in Biomedical Engineering.

Department of Biomedical Engineering

Thesis Advisor:	*Dr. Bruce P. Lee*
Committee Member:	*Dr. Jingfeng Jiang*
Committee Member:	*Dr. Patricia A. Heiden*
Department Chair:	*Dr. Sean Kirkpatrick*

Contents

List of Figures

List of Tables

Preface

Approximation of damaged tissues with a view of restoring their morphology and functionality is the prime motive of surgical procedures. Current trends in surgical procedures involve the wide use of wires, sutures and staples for repairing the injured tissues. These practices require highly trained surgeons and other personnel not to forget the possibility of additional trauma to the surrounding tissues or organs. The concept of surgical adhesives is emerging as a promising alternative and a possible substitute for the currently employed techniques. Certain formulations of these adhesives have been demonstrated as proof-of- concept while some have made it to the Operation Rooms. Facile adhesive bonding is an important phenomenon not only in the field of biomedical engineering, but also in many other pivotal research areas like automotives, aerospace, aeronautics, electronics and so forth. For the surgical application in particular, quite often, there is a need for strong and temporary adhesion for the reconstruction of damaged tissues or organs. What sets the surgical scenario aside from some of the aforementioned categories is the requirement of adherence to tissues in a wet environment. As the majority of the tissues in the body are composed mainly of water, effective adhesion under wet conditions is an ideal property that a surgical adhesive needs to possess. Of late, substantial research has been conducted in the smart polymer adhesives category in an effort to introduce a bioadhesive that can adhere to a variety of substrates of interest under wet conditions. One such

leading research efforts is the sub-category of smart polymer hydrogel adhesives that are inspired by mussel adhesive proteins (MAPs). Marine mussels secrete a series of proteins[2] in their foot that enable them to attach, bind or adhere themselves to rocks and other substrates in rough, intertidal zones. These hydrogels employ dopamine methacrylamide (DMA), a synthetic derivative of mfp-3 (Dopamine), as the adhesive element in a polymer network. Its adhesion to inorganic substrates like glass, mica and titanium is dictated by hydrogen bonding [3], [4] ,[5], [6], [7]. However, it has been observed that oxidation of the catechol groups that are responsible for interfacial binding has a detrimental effect on the adhesive performance with respect to adhering to inorganic substrates due to the formation of o-quinones[8], [9], [10] In order to tackle this issue, we have developed a model adhesive system that can be used to characterize the adhesive contact between a polymer hydrogel adhesive and a rigid substrate of interest.

Acknowledgments

I would like to thank my advisor, Dr. Bruce P. Lee for his continued advice on numerous topics in this project. His guidance played a pivotal role in the steering this project in the right direction. I would also like to thank all my colleagues who spent their valuable time in helping me whenever I faced obstacles in my experiments; and maintanied an inspiring atmosphere in the laboratory. I would also like to thank Dr. Jingfeng Jiang, Brett Barker and Matthew Clisch for their contribution in helping me develop the contact mechanics setup. I'm thankful to Dr. Patricia A. Heiden for serving on my committee. I'm grateful to to Dr. Faith Morrison for permitting me to use the Rheometer facility in Chemical Sciences and Engineering. I was also supported in part by the Kenneth L. Stevenson Biomedical Engineering Fellowship in Summer 2014.

List of Abbreviations

ATR	Attenuated Total Reflectance
AFM	Atomic Force Microscopy
3-AAPBA	3- Acrylamido phenylboronic acid
DI	De-ionized
DMA	Dopamine Methacrylamide
DMPA	2,2-Dimethoxy-2-phenylacetophenone
DMSO	Dimethyl sulfoxide
DOPA	3,4 -dihydroxyphenylalanine
EWC	Equilibrium water content
FTIR	Fourier Transform Infrared Spectroscopy
G'	Storage modulus
G"	Loss modulus
HCl	Hydrochloric acid
JKR	Johnson, Kendall and Roberts
MAP	Mussel Adhesive Proteins
MBAA	Methylene bis-acrylamide
N-HEAA	N- Hydroxyethyl acrylamide
OR	Operation Room

TRIS	Tris(hydroxymethyl)aminomethane
UV	Ultra-violet
1 M	1 molar
μm	micrometer

Abstract

Smart hydrogel adhesives with tunable properties consist of adhesive moieties in the polymer network that respond to external stimuli like pH, temperature, etc. Responsiveness of smart adhesives to pH, in particular, is important because of the simple actuation mechanism and the ability to achieve facile bonding and debonding upon command. Covalently crosslinked hydrogel adhesives were prepared by employing an N-HEAA (hydroxyethyl acrylamide) backbone embedded with dopamine methacrylamide (DMA), a marine mussel inspired adhesive protein and 3-acrylamido phenylboronic acid (AAPBA), to determine the effect of pH on the interfacial binding properties of the hydrogel adhesive with a borosilicate glass substrate. Swelling tests were performed to determine the response of the synthesized hydrogels to changes in pH values. These tests revealed that in a pH 3 buffered solution, hydrogels containing DMA and AAPBA showed a shrinking trend, while at pH 9, a swelling phenomenon was observed. The evidence from oscillatory rheometry tests exhibited elevated loss moduli (G') for hydrogels with DMA and AAPBA at pH 9, when compared to the relevant controls. In conjunction, the data from swelling tests and rheometry explained the unusual swelling of the hydrogels and formation of the catechol-boronate complex at pH 9, which caused more than an order of magnitude of increase in the G'' owing to the viscous dissipation of energy at that pH as compared to the control gels. The interfacial binding properties were tested by performing contact mechanics tests, in

the presence of an acidic/basic medium. The maximum work of adhesion values of $0.59 mJ/m^2$ were obtained for hydrogels with 2.5mol% DMA and 10mol%AAPBA in the polymer network, when tested against a borosilicate glass surface wetted with $250 \mu L$ of the pH 3 solution. At pH 9, this value reduced to as much as $1/5th$ of its value at pH 3. Earlier works have proposed that the oxidation of the catecholic groups that are chiefly responsible for adhesion with an inorganic substrate, is a deterrent to the adhesive properties of a hydrogel. We have accomplished the development of a model adhesive system in which we utilized the pH responsiveness of the hydrogels to demonstrate the elevated and reduced works of adhesion at acidic and basic pHs respectively. We believe that the catechol- boronic acid complex at pH 9 will allow for the reversible DOPA- facilitated adhesion. Reversibility studies performed in this direction revealed that while the hydrogels could recover their shape in terms of the measured diameters, further testing and analysis is required for understanding the ideal composition of the hydrogel and environmental trigger to actuate reversibility.

Chapter 1

Introduction

Bonding and debonding upon command while causing minimum damage to the conjoint materials involved is a desirable characteristic for an adhesive, especially in the field of biomedical engineering, like facilitating the painless removal of lesion dressings, complex structures for implants [11], [12], [13]. Even in the automobile industry, aeronautics, and other such fields, non-destructive bonding and debonding is being sought after to enable easier, safer and a more sustainable means for the assembly and disassembly of components [14]. The smallest of forces used for separation can become relatively large when it comes to delicate entities like cells, tissues, organs, etc [15], [16],[17]. The motivation for this project is the development of hydrogel based adhesives that have the potential to be used in the biomedical engineering field as in a plethora of other diverse applications. Current research in this field have led to the

development of adhesives that are majorly limited by the need for extreme conditions that cause debonding from the structure[14], or even more commonly, diminished adhesive prowess under wet conditions[12].

Certain arthropods, vertebrates and mollusks in nature have the unique capability to attach to a substrate upon will and detach from the same as and when required. Marine mussels secrete an amino acid- 3, 4-dihydroxyphenylalanine (DOPA), which imparts adhesive properties that are not diminished in the presence of water. They use this technique primarily for locomotion and anchoring themselves to a substrate by means of the catecholic side chains present in the amino acid. The adhesive fluid secreted in the foot of these mussels undergoes a biologically- triggered cross linking mechanism which converts the fluid into a solid glue, enabling its multifaceted adhesion to wood, metallic, and rocky surfaces, and protects it from crushing waves and tides. While wetting of the glue can be one of the major parameters that upset the adhesion phenomenon, MAPs with their innate ability to adhere to almost anything in a wet environment help us overcome this limitation.

These features are of particular interests to scientists as the design bio-inspired materials for the benefit of mankind. This phenomenon is of particular interest to us. We plan to use this wonder of nature and incorporate it into our nature inspired-adhesives.

There have been multiple studies related to the adhesion capabilities of mussel- inspired hydrogel adhesive in a wet environment[3]. There is some proof which suggests that the adhesive properties of the MAPs are greatly hampered upon oxidation of the catecholic species [18] that mediate adhesion with inorganic substrates like wood, metals, rocks etc. The goal of this project was to formulate a hydrogel with mussel inspired adhesive protein which binds to a substrate in the acidic medium (pH 3-4) and releases itself upon changing the pH to a basic value (pH 9-10). In an acidic medium, the catechol groups would be freely available for interfacial binding with an inorganic/organic substrate , see figure 1.1 . The presence of AAPBA acts as a protecting mechanism for the catechol groups against oxidation by the formation of a boronate-catechol complex. It has been previously researched that boronic acids have the ability to form reversible bonds with catechol and catechol substituted diols [19]. We exploit this complexation mechanism to develop hydrogels than can potentially bond and debond with respect to a substrate material reversibly, upon command.

pH responsive hydrogels is a subset of stimuli responsive hydrogels in which conformational changes in volume occur in the polymer network in response to the changes in the pH of the solution that it interacts with. It has been previously reported that when the pH of the interacting solution is lower than the pKa of the hydrogel (i.e the compound the hydrogel is composed of), the end groups tend to get protonated and this results in low osmotic pressure within the hydrogel network [20]. On the contrary, increasing the pH to a value higher than the pKa of the hydrogel causes

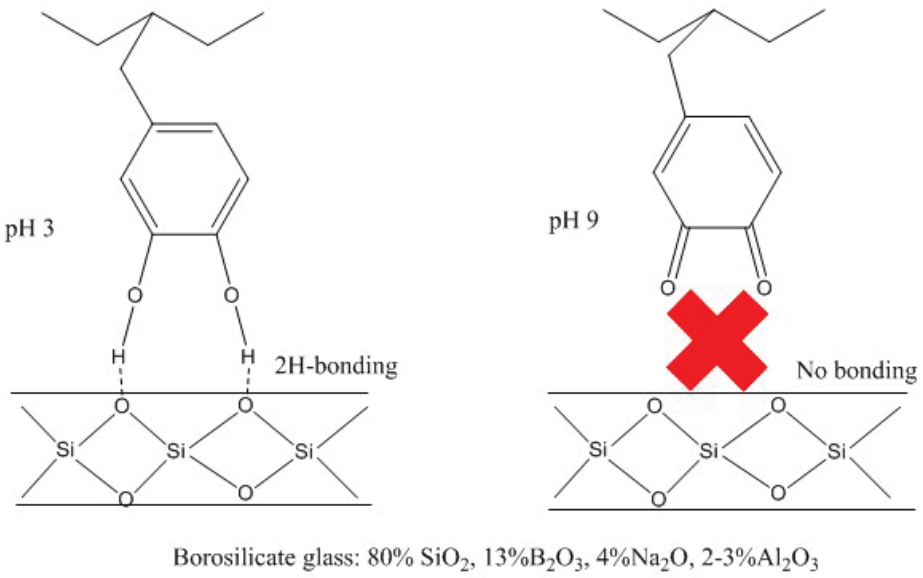

Figure 1.1: (a)The interaction of the catecholic functional groups with glass at pH 3, (b)formation of o-quinone, a deterrent to adhesive interactions

it to carry an overall negative charge which leads to a high osmotic pressure. This eventually results in the swelling of the hydrogel. In a study by Hussein Omidian et al.[21], it was demonstrated that the total charge on the polymer chains is an important parameter that is responsible for electrostatic repulsion due to presence of like charges. Being a reversible phenomenon, it allows for controlling of the hydrogel′s response by modulating the pH of the solution with which it interacts.

The interaction of the functional groups within the polymer is controlled by controlling the composition of the reactants in the precursor solution while the interaction between the hydrogel and the solution is governed by the properties of the solution

(here, mainly pH) and the responsiveness of the hydrogel is characterized by equilibrium swelling tests. The microstructure and the viscoelastic properties of the proposed adhesive were evaluated using rheological analyses. FTIR was as finger-printing technique to detect the presence of the expected functional groups at particular pHs. The interfacial binding of the hydrogel adhesive with respect to borosilicate glass was determined using a custom built Johnson, Kendall and Roberts (JKR) contact mechanics setup.

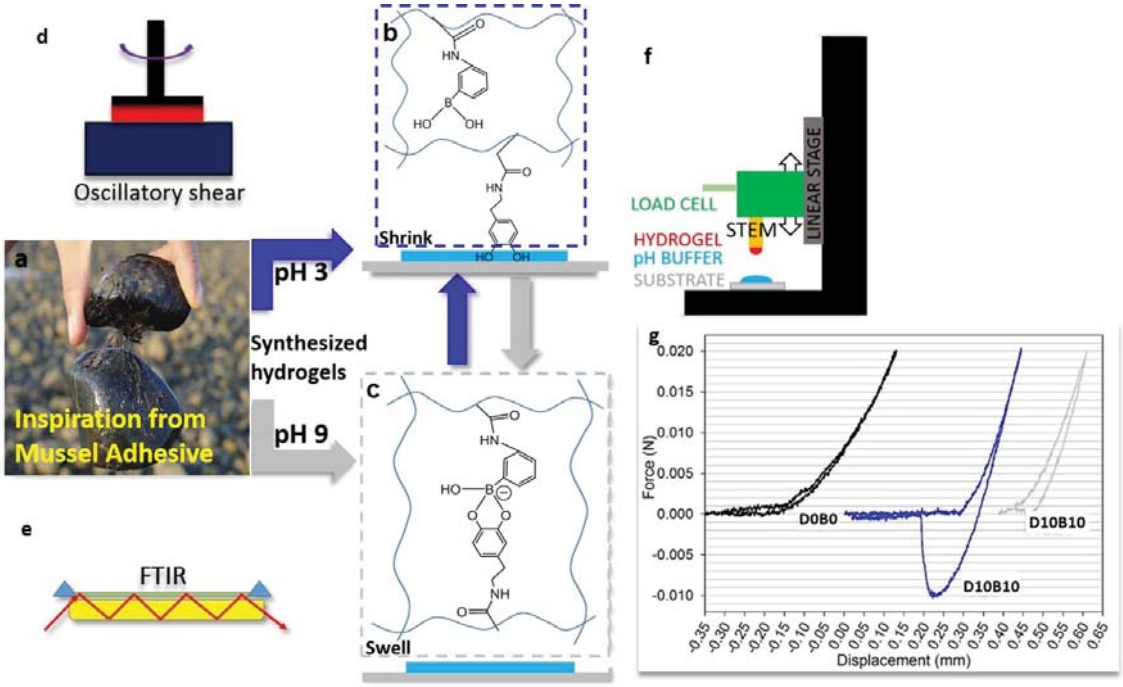

Figure 1.2: An overview of the study: (a) A mussel attached to a clay slab via byssal threads. After synthesis, the hydrogel adhesives were immersed in (b) a pH 3 buffered solution which causes the hydrogels to shrink and (c) a pH 9 buffered solution in which the hydrogels exhibit swelling behavior. They were further characterized using (d) Rheological analyses to probe their viscoelastic properties, (e) ATR- FTIR to determine the presence of desired functional groups, and (f) contact mechanics test setup to determine the interfacial binding of the hydrogel adhesives and (g) results comparing the elevated and reduced adhesive interaction, of DMA and AAPBA (10mol%DMA+10 mol%AAPBA=D10B10) containing hydrogels [in contarst to control (0mol%DMA and 0 mol% AAPBA black)=D0B0], with a borosilicate glass substrate in presence of acidic (blue) and basic (grey) pH environments.[1] C.

Chapter 2

Materials and Methods

2.1 Materials

N-Hydroxyethyl acrylamide(N-HEAA), 3-acrylamido phenylboronic acid(AAPBA) were purchased from Sigma-Aldrich, 2,2-dimethoxy-2-phenylacetophenone (DMPA) was purchased from Acros organics, methylene bis-acrylamide (MBAA) was purchased from Acros organics, dimethyl sulfoxide(DMSO) was purchased from Macron, distilled water, ethanol (190 proof) was purchased from Pharmco-Aaper and dopamine methacrylamide(DMA) was synthesized in our laboratory in accordance with a protocol published in [22].

2.2 Synthesis of hydrogel

N-HEAA (1M) was used as the monomer backbone to incorporate varying compositions of DMA and AAPBA to be dissolved in (40 v/v%) DMSO and DI water combination in a round bottom flask with a flow control adapter. 3 mol% of the bi-functional crosslinker MBAA was added to polymerize the N-HEAA. This setup was sonicated (Ultrasonic cleaner FS30, $42kHz \pm 6\%$, Fisher Scientific, PA) in a bath for 3 minutes to ensure the complete dissolution of the reactants in the solvent. After sonication, 0.1mol% DMPA was introduced into the round bottom flasks and the precursor solutions were placed in the freezer for 45 minutes. (All mol% as can been seen in table 2.1 are relative to 1M N-HEAA). Upon retrieval, they were back-filled with N_2 to remove the oxygen and were later maintained under vacuum and placed into a custom-built nitrogen rich chamber. Within the chamber, $50\mu L$ of the precursor solutions were carefully pipetted onto hydrophobic glass slides coated with (1H,1H,2H, 2H)-perfluorooctyl trichlorosilane to form hemispherical hydrogels upon UV- initiated curing in (XL-1000, Spectronics Corporation, Westbury, NY) for 600 seconds. After synthesis, the samples were immersed in measured volumes of pH 3 (DI water and 0.1M NaCl) and pH 9 (TRIS) buffers. For the rheological analyses swelling and reversibility tests, the precursor solutions were pipetted into customized molds formed by using 2 mm thick spacers as described in our previous works [23]. They were cut into discs, 15 mm in diameter and were nutated (using the Gyromini

Table 2.1
Compositions synthesized

Composition	DMA (mol %)	AAPBA (mol %)
D0B0	0	0
D2.5B0	2.5	0
D5B0	5	0
D10B0	10	0
D0B2.5	0	2.5
D0B10	0	10
D10B10	10	10
D5B10	5	10
D10B2.5	10	2.5
D2.5B10	2.5	10

nutating mixer, Labnet International, Inc.) for 48 hours to ensure the homogenous distribution of the medium prior to further testing. The table 2.1 summarizes the various compositions of gel synthesized along with some of the parameters that were tested.

Chapter 3

Characterization

3.1 FTIR

The sample compositions were freeze- dried for 4 days in a freeze-drier(Labconco)before crushing them into fine powder using a mortar and pestle. They were anlayzed using a Perklin Elmer Frontier Spectrometer fitted with a GladiATR^{TM} accessory from Pike Technologies. The wavenumbers at which characteristic functional groups were detected and tabulated.

3.2 Equilibrium swelling tests

The hydrogels were synthesized according to the aforementioned protocol. The 2mm sheets were cut into discs, 15 mm in diameter and were placed in scintillation vials containing 5mL of the acidic and basic buffered solutions. The hydrogels were allowed to equilibrate for 48 hours and were also nutated simultaneously to ensure good distribution of the solution. At the end of 48 hours, they were checked for swollen weights by withdrawing the mediums using a pipette and using kimwipes to dab the excess solution from the surface of the hydrogels. Once the weighing procedure was done, the hydrogels were first dried under vacuum and then freeze dried for at least 48 hours and then weighed again for dry weights.

3.3 Rheometry tests

The hydrogels were synthesized using the aforementioned protocol. The gels were compressed using a 20 mm diameter parallel plate geometry and subjected to 8% strain at a constant gap of $1800\mu m$. The storage (G') and loss (G'') moduli for varying compositions of the hydrogel were studied in the frequency range of 0.1-100 Hz. Oscillatory shear was employed using TA Discovery Hybrid Rheometer-2 (TA Instruments) to characterize the viscoelastic behavior.

3.4 Contact mechanics

In order to determine the interfacial binding and the effect of boronic acid- catechol complexation on adhesive property of the hydrogel adhesives, Johnson, Kendall and Roberts (JKR) contact mechanics test was performed using a custom-built indentation mechanism [24]. An illustration of the setup is shown in 3.1. The ALS-06 load stem from Transducer Techniques was used as a base for affixation of the hydrogel. A precision 10 gram load cell (Transducer Techniques), calibrated for applying compressive loads was used in conjunction with a high resolution (minimum incremental motion of $0.1\mu m$ steel linear stage stepper motor (Newport) for recording the forces and the displacement data respectively. The Virtual Instrument Software Architecture (VISA) standard was used for configuring, programming, and troubleshooting the serial interface instrumentation (Single Axis motion controller by Newport). Borosilicate glass (Capitol Brand ® M3504-1F Microscope slides) slides were used as the substrate to test the adhesive properties of the hydrogels. These slides were cleaned with ethanol (190 Proof, Pharmco-Aaper) and DI water before every contact. Cleaning of the substrates is important so as to avoid the presence of any ionic debris that could cause contamination and eventually hamper adhesion. Also, new slides were used for each of the two pHs tested (when a switch was made). The hemispherical hydrogels (synthesized as described in the Experiments section) were equilibrated in the pH 3 and pH 9 buffers for 48 hours.

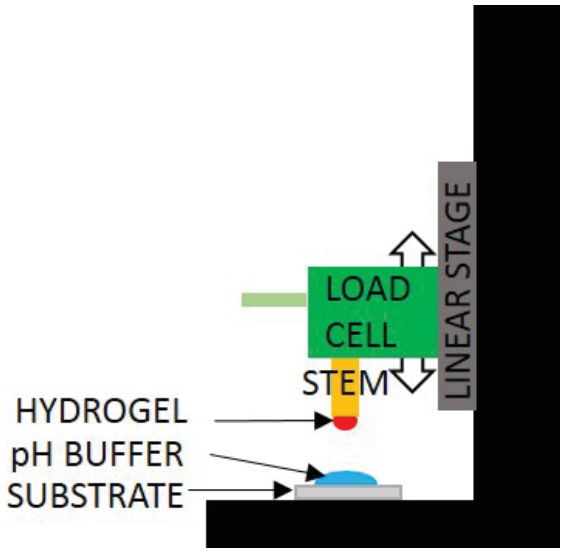

Figure 3.1: Representative illustration of the contact mechanics setup

The hydrogel adhesive sample was fastened to the load cell stem using superglue (Loctite Professional Liquid) and was allowed to form a bond for 4-5 seconds. Prior to the start of each test, the gel was allowed to regain its swollen state (time allowed 10 sec) by allowing its contact with $250\mu m$ of a freshly prepared pH buffer [25], identical to the one in which it was immersed for 48 hours. At this point, the hemispherical gel is close to, but not touching the substrate. The sample is then indented towards the substrate at a constant speed of $1\mu m/sec$. Once a preload of 20mN was reached, using the LABView program, the sample was retracted at the same speed till a force of approximately 0mN was recorded. For the instances that involved tensile forces as a result of the pull-off forces, the tests were continued until a force of approximately 0mN was recorded after the pull-off forces were registered. Load (P) versus displacement (δ) curves were plotted and analyzed to deduce the maximum pull-off forces, and work of adhesion values. The approach part of the curve was

used to determine the Young′s modulus. The height (h) of the hydrogels and base radius (r) were measured using digital vernier callipers before the start of each test. The maximum pull-off forces in the negative direction of the Y-axis and the work of adhesion values calculated by integrating the area under the curve with respect to the appropriated maximum area of contact of the hydrogels with the substrate were recorded.

The approach part of the curve was fitted using the equation[26]

$$P = \frac{16R^{1/2}E\delta^{3/2}}{9} \tag{3.1}$$

where R is the radius of curvature of the hemispherical hydrogels, which is determined by their height (h) and base radius (r)[27].

$$R = h/2 + r^2/2h \tag{3.2}$$

Work of adhesion was calculated using equation [28]:

$$W = \frac{\int F d\delta}{A_{max}} \tag{3.3}$$

The approach part of the load versus displacement curve was fitted with a Hertzian model which relates the maximum displacement (δ) and the corresponding radius of

contact(a) [26], as:

$$\delta = \frac{a^2}{R} \tag{3.4}$$

3.5 Reversibility swelling and Rheometry studies

Hydrogels were prepared using the same protocol as was used for rheological analyses. 15 mm hydrogel discs were immersed in pH 9 for 48 hours. This was also equal to the time that these samples were nutated. At the end of 48 hours, the samples from pH 9 were rinsed with DI water and the excess water from their surface was blotted using kimwipes. These samples were then immersed in pH 3 and the nutating process was resumed and carried on for another 48 hours. At end of 48 hours, their diameters were recorded using a pair of digital vernier callipers and they were then tested for their loss and storage moduli. These samples were compared against hydrogels that were equilibrated and nutated at pH 3 and pH 9 for 48 hours.

3.6 Statistical analysis

Statistical analysis was carried out using JMP Pro 11 software, SAS Institute, NC. Student t- tests and one way analysis of variance (ANOVA) was performed for comparing the means of multiple groups. Values less than 0.05 were considered significant.

Chapter 4

Results and Discussion

This project was aimed at loading a neutral monomer with pH responsive components, viz. DMA and AAPBA, that would react to the changes in pH to achieve the desired functionality. Most importantly, the prediction of pH for complexation in order for the hydrogel to exhibit switchable adhesion would dictate the formation of the catechol-boronic acid complex. Lihong He et *al.*[29] have reported that the pK_a value of catechol is about 9.3. Jun Yan et *al.*[30] have also reported that the pK_a value of catechol is around 9.3 and that of phenylboronic acid is around 8.8. They suggested that for effective interaction between a diol and a boronic acid, the ideal value of pH is given by the equation $pH_{ideal} = (pK_a - acid + pK_a - diol)/2$. Hence, for our experiments, we choose $pH = (8.8 + 9.3)/2 \approx 9$ as the ideal pH to observe the complexation between the DMA and the AAPBA components [31], [32].

4.1 FTIR Results

FTIR was used as a fingerprinting technique to confirm the presence of the expected functional groups and also to characterize the formation of new bonds as a result of the complex. The FTIR spectrum of D10B0 at pH 3 exhibited the characteristic groups -OH, the secondary amide bonds -NH- and C=O in the frequency range of 3400-3000, 1600-1500 and 1680-1630 cm^{-1} respectively. At pH 9, similar peaks were observed for D10B0. At pH 3, D0B10 exhibited the -OH, secondary amide bonds -NH- and C=O and the m- substituted benzene bonds in the frequency ranges 3400-3300, 1500-1400, 1680-1650 and 800-700 cm^{-1} respectively. D0B10 exhibited a similar structure at pH 9.

The striking difference in the peaks observed was in the testing group of hydrogel adhesives D10B10 at pHs 3 and 9. At pH 9, D10B10, a characteristic peak was observed at $1500cm^{-1}$ which was not present in either of D10B0 or D0B10, see figure 4.1. Moreover, it was not present in D10B10 at pH 3. We believe that this peculiar peak translates to the benzene ring stretch in aromatic compounds, likely to be a result of change in vibrational state, caused by formation of the complex and the rearrangement of atoms. In the work published by George C. Chen [33],the formation of a borate-catechol complex has been reported in the frequency range of 1478-1501 cm^{-1} which is in accordance with our observations.

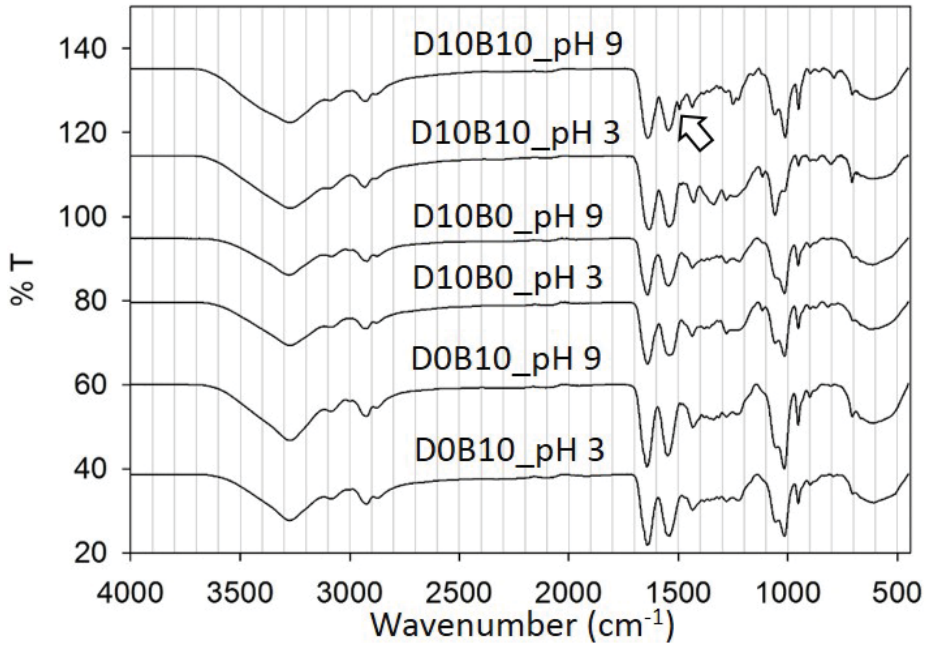

Figure 4.1: FTIR spectra of the tested hydrogels

4.2 Swelling ratio tests

The control hydrogels with 1 M N-HEAA backbone did not exhibit any significant changes in its network in response to the alteration of the pH values; see figure 4.2. This enabled us to provide a neutral, hydrophilic- polymer backbone to observe the effects of pH on introduction of the adhesive and protective moieties resulting in the intended pH responsive hydrogels. Increasing DMA content decreased the swelling ratio of the hydrogels; figure4.2. This is likely attributed to the increased hydrophobicity of the network caused by the benzene ring in DMA.

In accordance with the electronic theory of repulsion, the excessive positive charges in

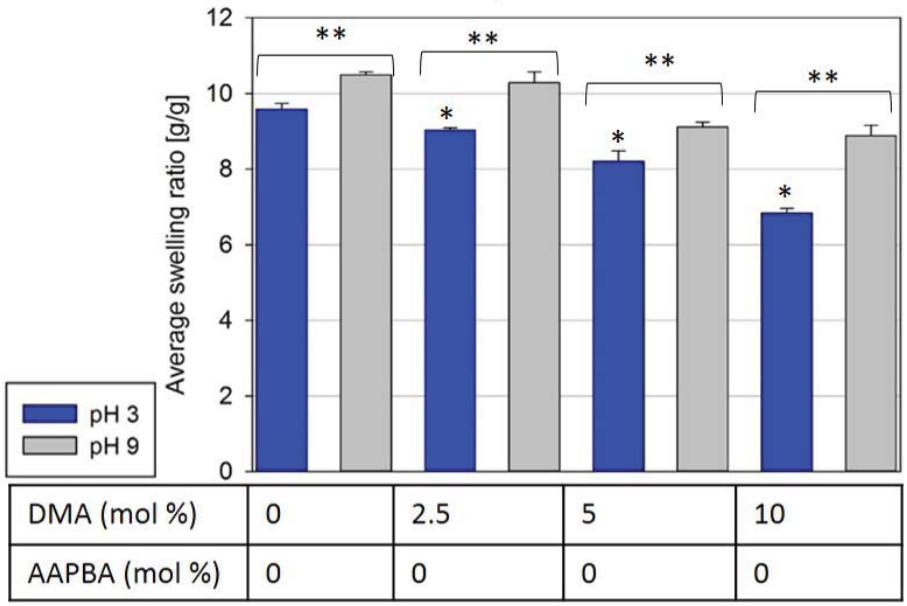

Figure 4.2: Effect of increasing mol % of DMA on the swelling ratio of the hydrogels: Adding increasing amounts of DMA into the polymer backbone caused an increased shrinking of the samples at an acidic pH, while at a basic pH, the swelling was comparatively higher. **p $<$ 0.01, *p $<$ 0.0001 in relation to D0B0.

the acidic HCl-NaCl buffered pH3 medium would cause the shrinking of the hydrogel network due to the interaction of the free catechol (OH^-) with the freely available H^+ ions from the solution that was used for equilibrating the hydrogel adhesives. On the other hand, in a basic medium, the oxidized catecholic groups repel the abundant OH^- ions provided by the TRIS-HCl buffer at pH 9. Qualitative evidence(from photographs in figure B.7) indicate that the hydrogels with the maximum catechol content i.e 10 mol% were evidently shrunken in pH 3 compared to the control samples that did not contain any DMA. The addition of increasing amounts of DMA also means that at a basic pH, the formation of semiquinone and quinone [9], [34] would be the most of all experimental combinations and would cause maximum apparent

repulsion upon formation of the unsaturated double bonds.

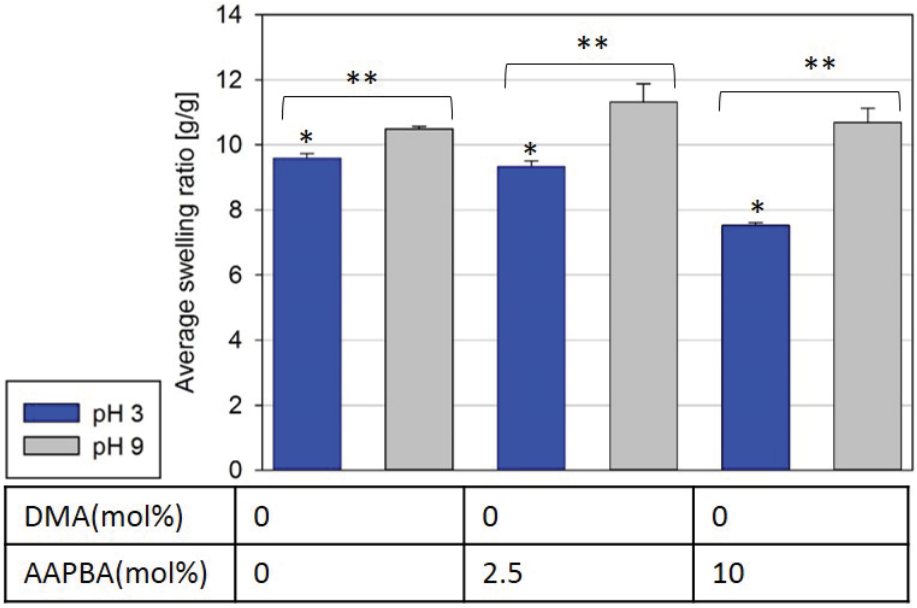

DMA(mol%)	0	0	0
AAPBA(mol%)	0	2.5	10

Figure 4.3: Effect of increasing mol % of AAPBA on the swelling ratio of the hydrogels: Hydrogels with elevated levels of AAPBA in the polymer matrix exhibited a shrinking effect in the acidic medium, while at a basic pH, they showed an exceptional swelling behavior. **p < 0.05, *p < 0.0001 in relation to D0B0.

It was interesting to note that addition of increasing amounts of AAPBA, as can been seen from figure4.3 has a consistently decreasing swelling trend in the acidic medium, which may be a result of decreasing hydrophilicity, while in a basic medium it has exhibited exceptional swelling characteristics [35]. The electronic attraction between the protons in the acidic medium and the OH- could be responsible for the shrinking behavior. PBA has pK_a of 8.8 [30]and it transforms into a negatively charged trigonal structure at pHs above 8.8. Also, Arum Kim et *al.*[35] showed that increasing pH caused increased swelling of the AAPBA. The elevated pH values present more OH^- ions to the AAPBA and it results in the conversion of the trigonal structure into a

tetrahedral one, see figure 4.4.

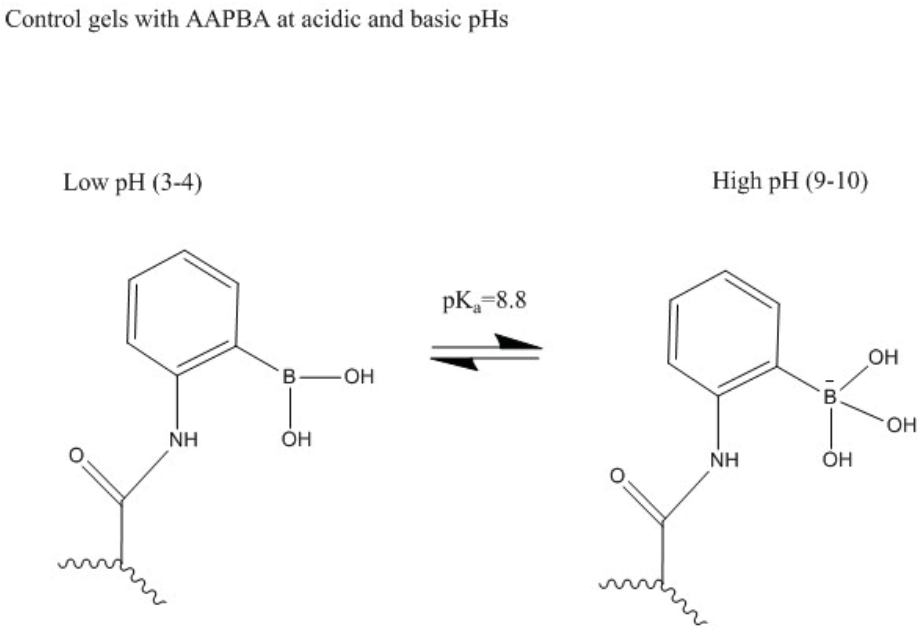

Figure 4.4: Figure showing the tetrahedeal moeity of AAPBA at pH values above thepK_a of PBA

The AAPBA controls swell to a larger degree as compared to the DMA controls which allows us to conclude that, at a basic pH, AAPBA is a charged moeity as compared to DMA under the same conditions. This also helps us conclude that the polymer backbone provides for an ideal mechanism of interaction of the pendant groups of the DMA and the AAPBA with the medium that is provided for equilibrating the hydrogels. The charges when balanced, cause a change in the polarity and add to the hydrophilicity of the hydrogel[35].

The complexation between the DMA and the AAPBA leaves a residual negative charge on the boron atom, refer figure 4.4. This means that as opposed to ordinary

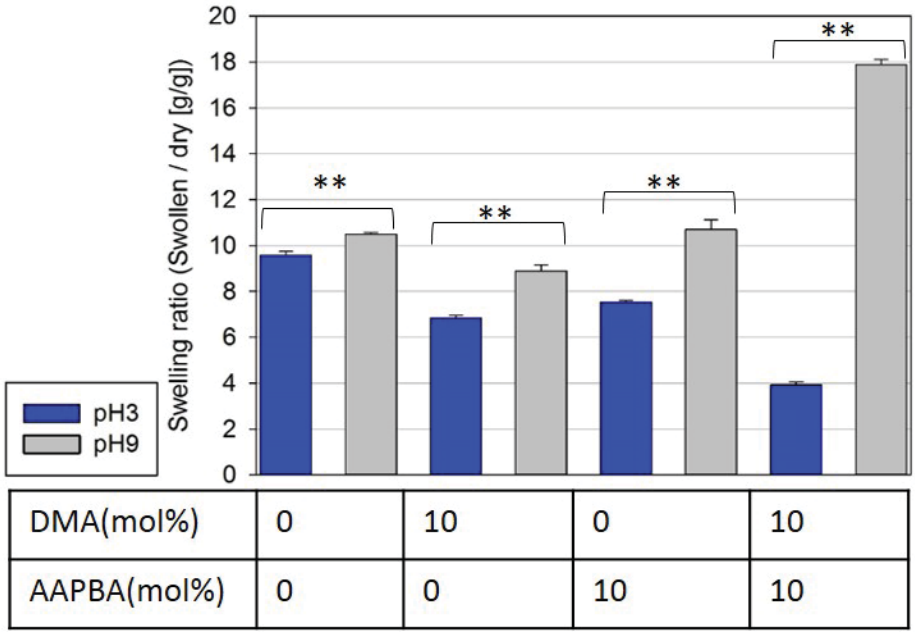

DMA(mol%)	0	10	0	10
AAPBA(mol%)	0	0	10	10

Figure 4.5: The swelling behavior of the testing set of hydrogel adhesives containing 10 mol % each of DMA and AAPBA in relation to its constituent control components. These hydrogels showed an upraised swelling in the basic medium when compared to either of the control sets immersed in the same environment for 48 hours. **$p < 0.05$

expectation that the hydrogels would be more densely cross linked and eventually shrink in a basic medium, the negative charges left on the boron atom cause repulsive forces to dominate the shrinkage that could possibly be caused by the newly formed, additional weak physical coordinate crosslinks. Maximum shrinkage in the acidic medium and maximum swelling in the basic medium in comparison to the other tested compositions was observed for D10B10. From figure4.5, it can be seen that the swelling for the 1:1 molar ratio of DMA: AAPBA was greater than the individual components involved. This supports the argument that the complexation causes the boron atom to carry a negative charge [35], [30], and as a result, adds to the total negative charge that is presented by the AAPBA moiety independently and

a 356.46% increase in average swelling ratio from pH3 to pH 9 was observed. For the same reasons, there was a 135.93% increase in average swelling ratio for D5B10 when the values at pH 9 and pH 3 were compared, see figure 4.6. For D2.5B10, the photographs taken showed that the complexation led to the DMA being well protected from oxidation (based on the intensity of the reddish-brown color, refer to supporting information provided by [29], refer to figureB.7. This meant that the excess AAPBA contributed to the hydrogels swelling 4.3. There was a 94.7% increase in average swelling ratio when the values for D2.5B10 at pHs 9 and 3 were compared. For D10B2.5 at pH 3 and pH 9, the swelling behavior of the AAPBA is dominated by the hydrophobic characteristic of the DMA. At pH 9, D10B2.5 showed a 93.67% increase in average swelling ratio in relation to pH 3, see figure 4.6. This indicates that fewer complexes were formed and as as a result, the cumulative negative charge caused by boron was comparatively less, which bears a direct relation to the number of crosslinks formed at acidic and basic pHs. At a basic pH, the bulk of DMA is oxidized because the reduced amount of AAPBA cannot provide enough protection against the oxidizing effect of the basic buffer. The uncomplexed DMA not only gets oxidized but it also means that the sample exhibited less swelling as a result of the reduced charges on AAPBA. This is evident from comparison of the swelling behavior of D0B2.5 at pH 9 with this particular composition. It can hence be inferred that reducing the DMA content in relation to the AAPBA led to a reduced swelling ratio when the pH was switched from 3 to 9.

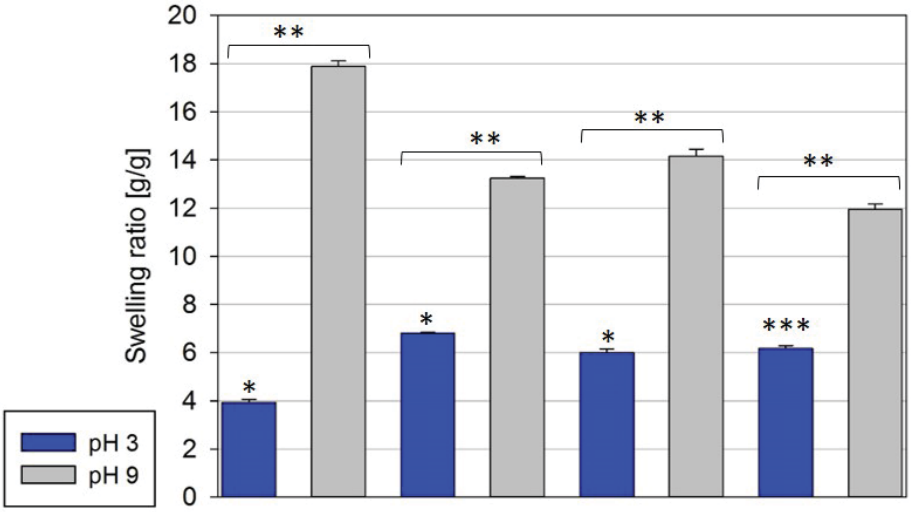

DMA (mol%)	10	2.5	5	10
AAPBA (mol%)	10	10	10	2.5

Figure 4.6: The average swelling ratio of the testing set of hydrogels containing varying ratios of DMA and AAPBA were determined in order to gauge the mechanical attributes and crosslinking densities of the hydrogels. *p < 0.05, **p < 0.0001. ***p $= 0.2222$ in relation to D5B10.

We believe that the formation of the coordination complex with the residual negative charge on the boron atom promotes the swelling of the hydrogel adhesives. Although the control group of AAPBA hydrogels were found to swell at basic pH values, the swelling observed as a result of the complexation for the testing sets was of higher magnitude. This is the mechanism which we propose to exploit for protecting the catecholic groups against oxidation, which has been widely documented as being a deterrent to catechols ability to bind to inorganic substrates.

4.3 Rheological analyses

Rheological analysis was used to confirm the formation of a complex. At an acidic pH of 3, the G' values for the control set comprising of D0B0, D2.5B0, D5B0, D0B2.5, D0B10 were all independent of frequencies in the lower frequency range up to 45 Hz. This indicates that the gels behave as covalently crosslinked ones in the specified frequency range. Also, the G' values were of an order of magnitude higher than the G'' values for the respective samples, which further elucidate that they are of elastic nature. It also suggests that the hydrogels can retain their microstructure across the range of frequencies up to 45 Hz. Beyond 45 Hz, the G' values are dependent on frequency, likely because the hydrogels do not get enough time to relax and retain their structure [36]. At pH 3, it was observed that adding increasing amounts of DMA into the HEAA backbone caused the storage modulus (G') to increase, see figure B.8. However, no specific trend was observed with respect to changing DMA concentrations and it's effect on the G'' values of the controls. at pH 3, the G' values for D0B2.5 were lower than those for D0B10, see figure B.9. This corroborates evidence from the swelling tests which indicated that the D0B2.5 gels swell more in an acidic medium when compared to the D0B10 ones. A similar trend was observed in their G' values at pH 9 B.11, which also was in accordance with the swelling data.

For D10B10 in comparison with controls D10B0 and D0B10

For the control hydrogel D10B0 at pHs 3 and 9, G' is independent of frequency in the lower range of frequencies up to 45 Hz, see figure 4.7.

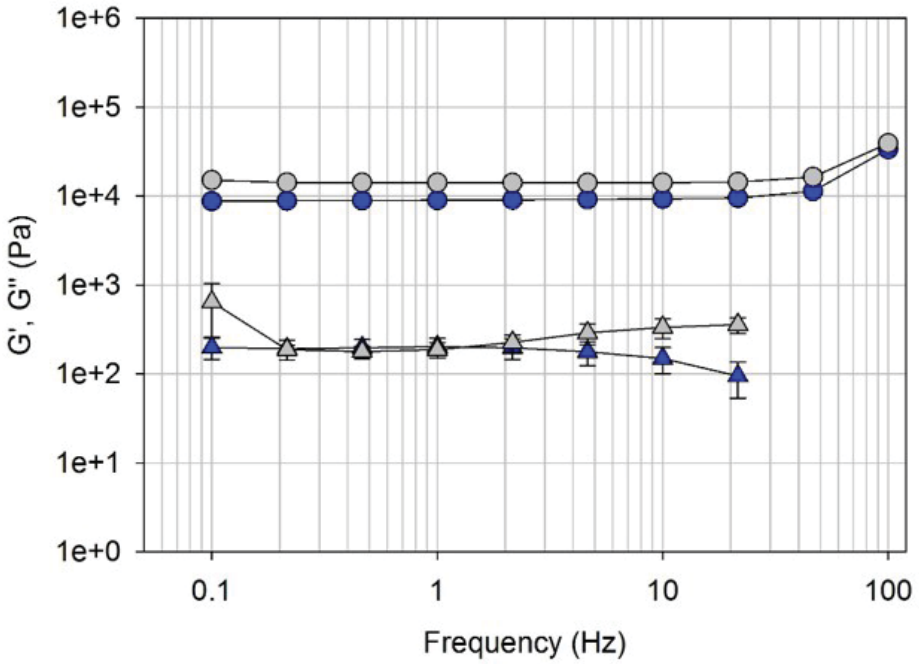

Figure 4.7: Comparison of G' and G'' values obtained from an oscillatory frequency sweep of the sample D10B0. The circles indicate G' while the triangles stand for G''. Blue color = pH 3, Grey color = pH 9.

The G' values are of an order of magnitude greater than the G'' values. These conditions indicate that the synthesized gels behave as covalently cross linked, elastic network. For the other set of control hydrogel D0B10 at pHs 3 and 9, see figure4.8, the same conditions hold true because of which they too, behave as elastic, chemically crosslinked gels that can maintain their structure.

Overall, the G' and G'' of the controls D10B0 and D0B10 show that the controls act as covalently crosslinked, elastic hydrogels with the G' values being independent of

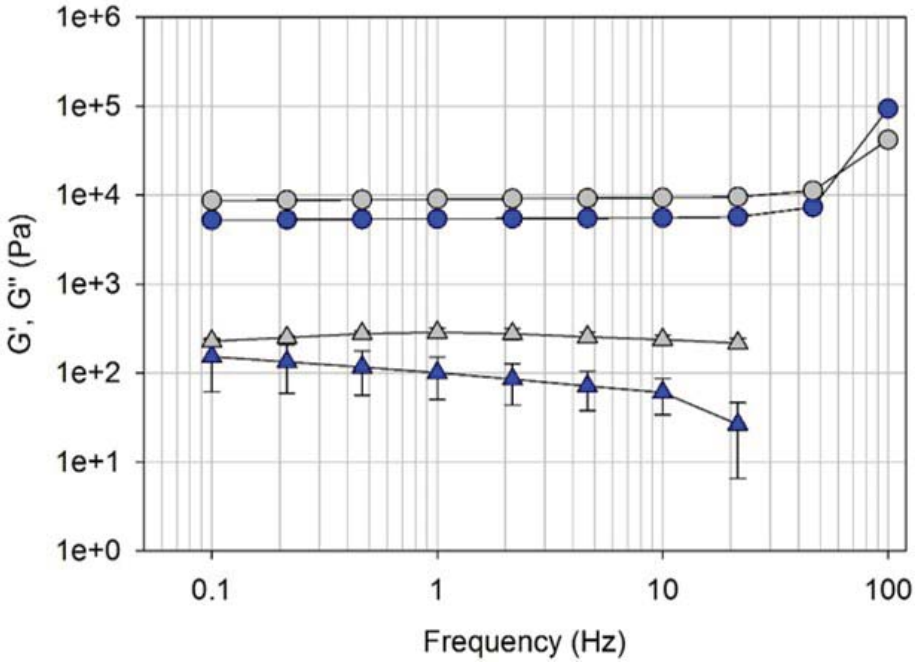

Figure 4.8: Comparison of G' and G'' values obtained from an oscillatory frequency sweep of the sample D0B10. The circles indicate G' while the triangles stand for G''. Blue color = pH 3, Grey color = pH 9.

frequency in the lower range of tested frequencies and also G' vlaues being more than an order of magnitude higher than G'' values.

At pH 3, D10B10 has G' values that are not dependent on frequency in the range of frequencies from 0.1-45 Hz. Beyond this, the oscillatory perturbations result in an irreversible change in the polymer microstructure as the hydrogels do not get enough time to retain their structure. Also, the G' values are more than an order of magnitude higher than G'' values, indicating that the composition is an elastic, covalently cross linked hydrogel adhesive. At pH 9, D10B10 displays a frequency- dependent trend for G' values in the range of 0.1-45 Hz ,see figure 4.9

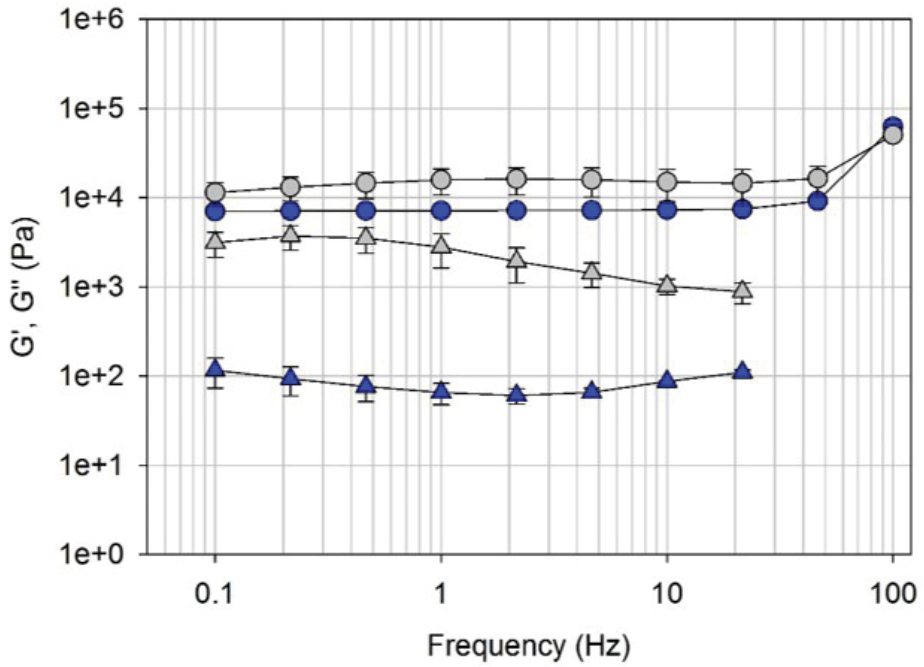

Figure 4.9: Effect of complexation on G' and G'': D10B10 showed frequency independent response in terms of G' values at pH 9, while it exhibited a dependence on frequency across the same range at pH 9. There was a striking increase in the G'' values from pH 3 to pH 9, most likely a result of the breaking of the physical coordinate bonds in the complex at pH 9. The circles indicate G' while the triangles stand for G''. Blue color = pH 3, Grey color = pH 9.

Storage and loss modulus for testing set at pH 3 and pH 9

The addition of DMA causes the hydrogels to shrink at pH 3. Addition of increasing amounts of AAPBA also led to decreasing swelling for the hydrogels at pH 3. The swelling ratios for the gels at pH 3 were significantly lower than that at pH 9. On account of the greater magnitude of swelling of the gels containing both DMA and AAPBA in pH 9, it was anticipated that their storage modulus would be lower than the same set of gels at pH 3. However, the formation of the catechol-boronic acid complex (boronate ester formation) results in inflated G' values at pH 9. We estimate

that this increase in the G' values is because of the new physical coordinate crosslinks in addition to the already existing chemically crosslinked polymer backbone.[37], [30], [29] and [38] showed that the formation of the complex leaves behind a negative charge on the participating Boron atom, producing an osmotic pressure difference, which can be thought of as the chief element responsible for the swelling phenomenon at pH 9 . Though statistically insignificant, there was a measured increase in each corresponding set of acidic and basic values of G' for the varying compositions of DMA and AAPBA. This trend is because of the presence of the physical coordinate bonds present between the catecholic end groups and the boronic acid. For frequencies beyond 45 Hz, there was a sharp increase in G' values which meant that the magnitude of oscillations was to high for the hydrogels to maintain their microstructure. D10B10 at pH 9 displayed an elevated G'' trend in comparison to G'' values for at pH 3, see figure 4.9. This is evidence for the dissipation of energy for the breaking of bonds and the resulting viscous dissipation of energy at pH 9.

Storage and loss moduli for varying compositions of DMA and AAPBA a pH 3 and pH 9

From the figures B.8, B.10 and B.11 it was evident that the controls, viz. the hydrogels containing DMA or AAPBA independently in the polymer network, behave as covalently cross linked hydrogels as their G' values are of an order of magnitude higher than the G'' values. Also, at pH 3, the storage modulus of the hydrogels containing

different molar ratios of DMA and AAPBA is higher than the corresponding G'' values, see figure B.12. This indicates that even the hydrogel containing a combination of the two moieties in its network behaves as a covalently cross linked hydrogel. The G' values are independent of frequency up to a frequency of approximately 40 Hz, indicating that above this frequency, the time provided for the hydrogels to relax and retain their structure was insufficient as a result the perturbing oscillations.

When the G' values of the hydrogels containing both; DMA and AAPBA at pH 9 were probed, it was found that a frequency dependent trend was observed from 0.1-1 Hz, see figure B.12, following which, the G' values were independent of frequency till approximately 40 Hz. Beyond 40 Hz, the frequency dependent nature of the curve means that at higher frequencies of oscillations, the network is unable to relax and retain its original structure. The frequency dependent trend from 0.1-1 Hz is an indication of the physical coordinate crosslinks formed as a result of the catechol-boronic acid complexation at pH 9, which can be concluded from the fact that no such trend in G' values is observed at pH 3. When compared to the relevant controls, an increased G'' value was seen in the corresponding hydrogels containing a combination of the control elements, see figure B.9. Also, from figure B.13 the G'' values at pH 9 were at least an order of magnitude higher than those for the corresponding set at pH 3.

4.4 Relation between the swelling and rheometry tests: Justification for stitching together the evidence from swelling and rheometry

The distribution of crosslinks in a covalently cross linked hydrogel is usually not uniform. Certain areas within the hydrogel are densely cross linked while in some other areas the crosslinking is sparse [39]. The densely cross linked regions are the zones where the aggregation of the crosslinker causes the hydrogel to become more hydrophobic as compared to the other regions. In the case of our hydrogels, at pH 3, the chemically cross linked control and testing set of hydrogels exhibit an overall hydrophobic behavior as compared to the ones at pH 9. However, at pH 9, the testing set of hydrogels containing both DMA and AAPBA tend to form boronate ester complexes which causes an increased swelling phenomenon, predominantly because of the boron atom that is left with a negative charge at the end of the complexation [38]. This negative charge promotes the excessive swelling of the hydrogels containing AAPBA at pH 9. The data from rheological analysis also shows a slight increase in the G' values at pH 9 on account of formation of the new coordinate complexes. In addition, there is a nominal frequency dependence observed for the testing set of hydrogels in which the protective complex was hypothesized to be existing.

Table 4.1
Summary of the average swelling ratio, G′ and G" at 10 Hz for the tested compositions of hydrogel adhesives

Composition	Average swelling ratio [g/g] (n=3)		G' (Pa) at 10 Hz (n=3)		G" (Pa) at 10 Hz (n=3)	
	pH 3	pH 9	pH 3	pH 9	pH 3	pH 9
D0B0	9.58±0.15	10.49±0.08	8130.48±349.48	8282.83±163.00	162.24±22.98	527.02±218.62
D2.5B0	9.03±0.07	10.28±0.29	9750.13±62.611	6885.45±1153.43	163.79±43.24	406.94±112.96
D5B0	8.21±0.27	9.11±0.13	6151.40±310.51	6120.36±166.49	37.48±2.62	451.68±78.39
D10B0	6.84±0.12	8.89±0.27	9299.71±278.63	14164.7±590.31	149.01±48.56	332.54±83.34
D0B2.5	9.34±0.17	11.31±0.57	4607.51±128.80	5547.93±188.96	30.97±2.40	116.65±72.27
D0B10	7.53±0.08	10.69±0.43	5560.29±179.06	9333.95±287.83	60.33±26.5	237.37±29.33
D10B10	3.92±0.14	17.88±0.23	7288.41±507.09	14940.64±5939.13	86.98±1.37	1020.06±201.15
D5B10	6.01±0.14	14.16±0.29	8222.11±106.74	18863.77±2199.92	54.82±7.11	678.26±111.25
D10B2.5	6.16±0.13	11.94±0.24	6971.32±231.51	12507.47±1562.53	41.51±2.42	233.63±18.78
D2.5B10	6.80±0.03	13.24±0.08	4148.45±260.38	12475.09±3596.35	27.57±2.83	528.59±94.67

The storage modulus (G') of the viscoelastic materials translates into the elastic component of the material. Generally, a material with higher G' values indicates a highly cross linked polymer network and represents an elevated stiffness of the material. At pH 3, the hydrogels containing varying compositions of DMA and AAPBA exhibit a lower G' as compared to the storage modulus at pH 9; see figure4.10. This is because at pH values below the pK_a required for the complexation of the major reacting components (DMA and AAPBA), there is no interaction between them.

At pH 9, the pH of the embedded elements is greater than the pK_a required for complexation. The consequent formation of the complex leaves a negative charge on the boron atom in the AAPBA. These negative charges interact with the excess

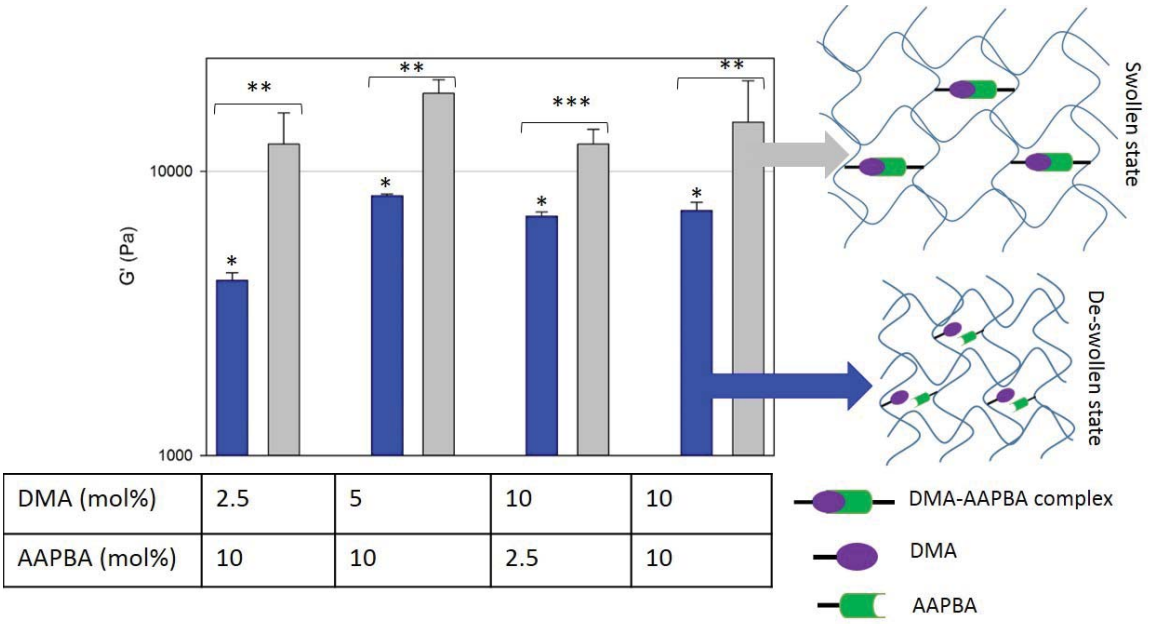

DMA (mol%)	2.5	5	10	10
AAPBA (mol%)	10	10	2.5	10

Figure 4.10: Corroborating the data from swelling and rheometry at 10 Hz: For the testing set of hydrogels, the storage modulus at pH 9 was significantly higher than that at pH 3. This was contradictory to our expectation that elevated G' values would actually be a result of fewer crosslinks in the polymer microstructure, eventually leading to reduced swelling. Blue = pH 3 and grey = pH 9. **p $<$ 0.05, ***p = 0.053, *p $<$ 0.0001

OH- ions presented at pH 9, causing the hydrogel to swell. The data obtained from rheomtery suggests that the physical coordinate crosslinks were formed as expected which result in an elevated G' at pH 9. However, the increment in the G' values is not a significant one. This is an indication that these crosslinks are not strong physical bonds. On an average there was a 2.2 fold increase in the storage modulus values observed over the varying compositions of DMA and AAPBA that were tested. The highest increase (3 fold) was observed in the D2.5B10, as can be seen in figure 4.11.

The loss modulus (G'') of viscoelastic materials is related to the viscous properties of the material. It indicates the ability of the polymer to dissipate the stored elastic

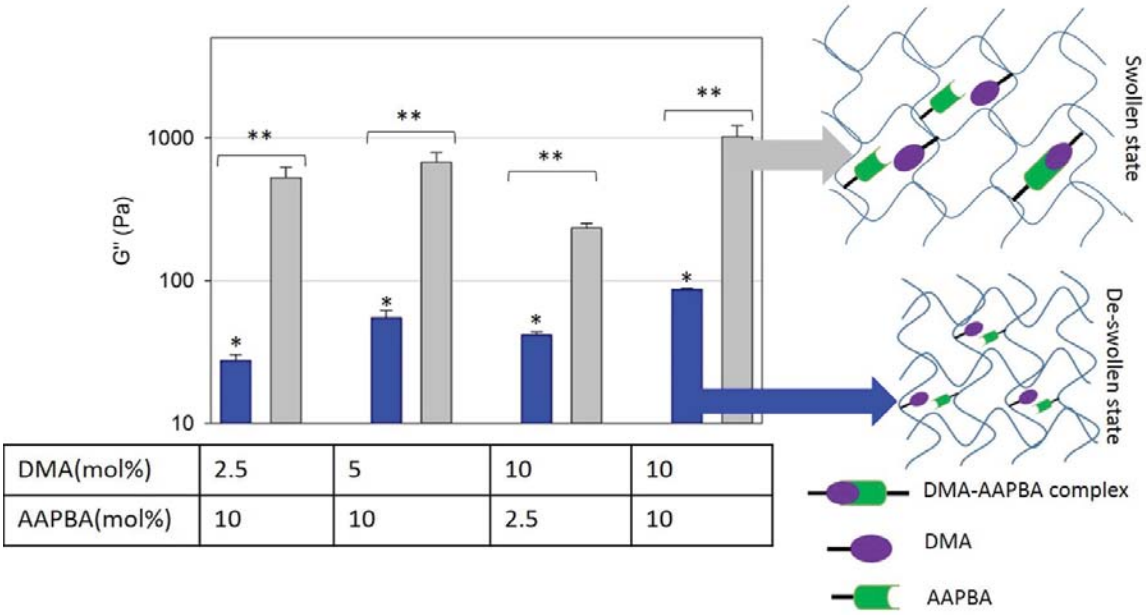

Figure 4.11: Corroboration of loss moduli of the testing sets of hydrogels at 10 Hz before and after complexation: There was more than an order of magnitude of increment in the G'' values for the hydrogels at pH 9 as compared to those at pH 3. at pH 9, the hydrogel adhesives still continue to remain in the swollen state, but the breaking of physical coordinate bonds causes an elevation in the G'' values. Blue = pH 3 and grey = pH 9. **p $<$ 0.05, *p $<$ 0.0001

energy upon deformation. At pH 3, the observed G'' values are significantly lower than the G'' values at pH 9. This is because when the microstructure of the hydrogel adhesive is perturbed at 10 Hz, the stored potential energy is dissipated within the polymer matrix. The varying compositions of DMA and AAPBA tested at pH pH 9 exhibited elevated G'' values on account of the breaking of the physical coordinate crosslinks at a pH which was greater than the pK_a required for complexation, as can be seen in figure4.11, see table 4.1 . On an average, there was an order of magnitude difference (11.66 fold) between the G'' values at acidic and basic pHs. The highest increase (19.17 fold) was observed for the D2.5B10 combination which corroborates

the evidence obtained from the elevated G'' values for the same combination, see table4.1.

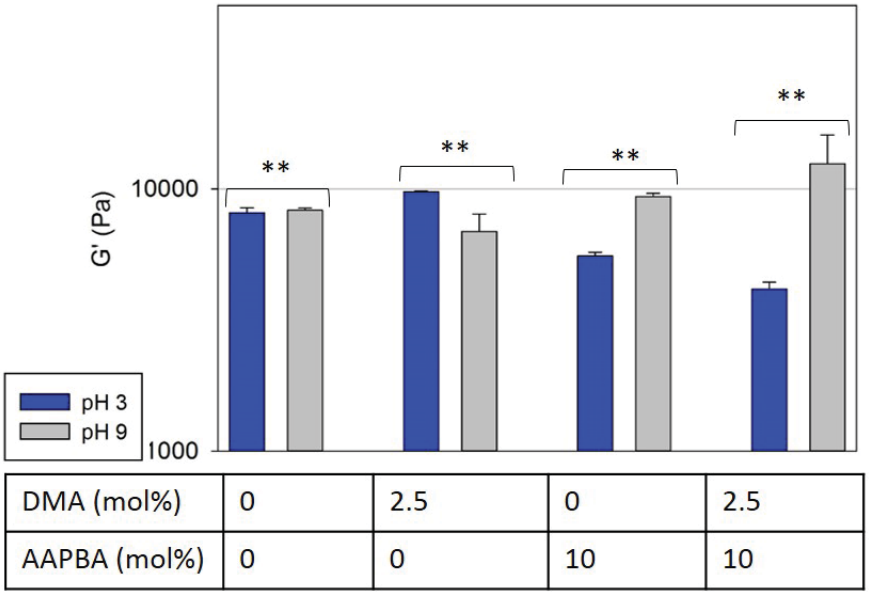

DMA (mol%)	0	2.5	0	2.5
AAPBA (mol%)	0	0	10	10

Figure 4.12: Comparison of G' of the control sets with testing set of hydrogels at 10 Hz: Increased G' values were observed for D2.5B10 at pH 9, owing to the formation of the complex which contributed to a higher increase in crosslinking, when compared to the controls, D2.5B0 and D0B10 at pH 9. **p < 0.05

This figure 4.12 shows the comparison of storage moduli of the control hydrogels with that of the testing set of hydrogels containing a combination of the control hydrogels. It can be seen that there is no statistically significant difference in storage modulus of HEAA hydrogels at acidic and basic pHs. For the hydrogels containing 2.5mol%DMA in addition to the HEAA backbone, a similar trend is observed. The hydrogels containing 10mol%DMA swelled to greater extent at pH 9 as compared to the swelling at pH 3. This is in accordance with the negative charge on the Boron atom that interacts with the excess of negatively charged ions provided by the pH 9

buffer solution, causing repulsion. The swelling is 1.68 times higher than the swelling observed at pH 3. At pH 9, the G' of the testing set of hydrogels is 3 times higher than those immersed in pH 3. The increase in G' values is a result of the physical coordinate crosslinks formed between DMA and AAPBA at pH values above the pK_a of the two interacting moieties. The increase in crosslinking density owing to the additional physical coordinate crosslinks contributes to the increased G' values.

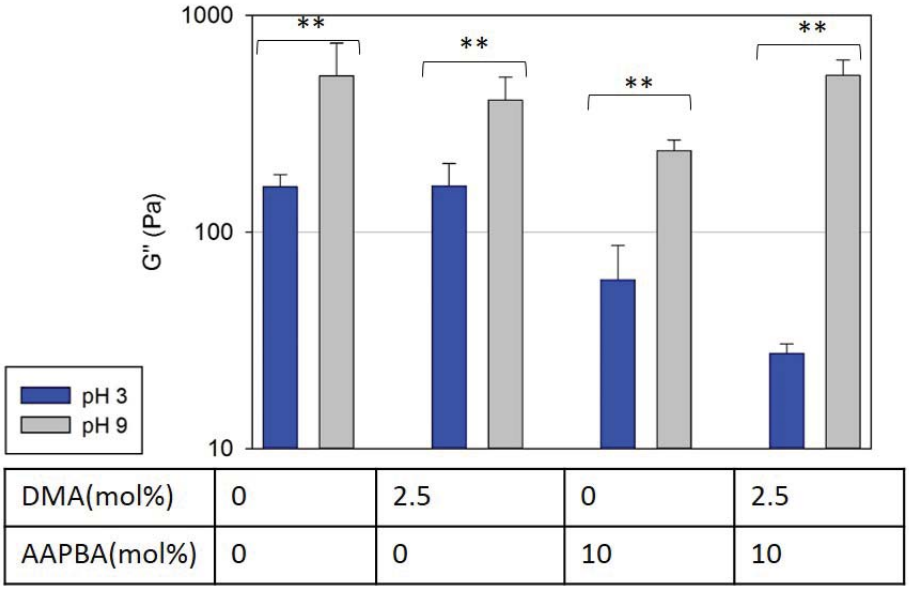

Figure 4.13: Comparison of G'' of the control sets with testing set of hydrogels at 10 Hz: Increased G'' values were observed for D2.5B10 at pH 9, because of breaking of the coordinate complex and the consequent dissipation of viscous energy, when compared to the controls, D2.5B0 and D0B10 at pH 9. **p < 0.05

At pH 3, the loss moduli of control hydrogels composed of the N- HEAA backbone is lower than the hydrogels at pH 9. The same trend is observed in the G'' of the control hydrogels D2.5B0 and D0B10. The maximum increase in the observed G'' values for the controls is in the case of D0B10. This could likely be because of the

transformation of the AAPBA in to a trigonal negatively charged compound. There is approximately a 4 fold increase in the measured G'' values for D0B10 at pH 9 as compared to those at pH 3. The most striking increase was observed in the case of the D2.5B10 at pH 9. A 19 fold increase was observed in the G'' values in the case of hydrogels containing this combination, see figure 4.13. This increase in the G'' values is a result of the breaking of the physical coordinate crosslinks formed at pH 9. It means that when the bonds break, the hydrogel adhesive is capable of dissipating the stored potential energy. This gives us strong evidence supporting our hypothesis regarding the formation of complexation between DMA and AAPBA.

4.5 Contact mechanics tests

Contact mechanics tests were first proposed in 1985 by Johnson, Kendall and Roberts (JKR)[40] and it deals with the study of materials while taking into account the precise geometry and substrate restrictions. According to this theory, the adhesive contact between the surfaces is related with not only the elastic properties of the material but also the interfacial binding strength. Since the contact between the material and the substrate is an adhesive one, it is expected that negative forces are recording during the pull-off period [41], [42], [43], [44],[45]. The contact mechanics curve is split into three sections for the ease of analysis. The point at which the sample first comes into contact with the substrate is followed by the loading of the

hydrogel with increasing forces at a constant velocity, until a fixed preload is reached. During this compressive regime, there is a change in the internal structure of the hydrogels. This part is called the approach curve. Secondly, once the preset load is reached, the hydrogel is withdrawn from the substrate at the same speed until a force of 0mN is recorded, which signifies the separation of the sample from the substrate. Finally, in case of an adhesive interaction, the forces in the negative direction of the Y-axis are referred to as pull-off forces and the maximum pull off force is the one that is recorded at maximum displacement, just before the hydrogel adhesive separates from the substrate.We use the JKR tests to determine the work of adhesion of the hydrogels which is the work done in releasing the hydrogels from the substrate by overcoming the interfacial binding energy between them. Additionally, the force versus displacement curves are also used to mathematically determine the Young′s modulus and the pull-off forces in the negative direction of the Y-axis. A summary of the results can be seen in the table4.2.

The average work of adhesion values for D0B0, the hydrogels devoid of any adhesive component, was $9.04E{-}2{\pm}2.05E{-}5mJ/m^2$. The average values for maximum works of adhesion for D2.5B0 and D10B0 were $5.42E-2\pm2E-5mJ/m^2$ and $1.64E-1\pm 5.8E-7mJ/m^2$ respectively. Also, at pH 3, the maximum pull off forces that were documented increased from $-2.10{\pm}7.09E{-}4mN$ for D2.5B0 to $-5.89{\pm}4.54E{-}4mN$ for D10B0; see figure4.14.

Table 4.2
Summary of the average work of adhesion, Young′s modulus and pull off forces for the tested compositions of hydrogel adhesives

pH	Composition (n=3)	Average Work of adhesion (mJ/m^2)	Average Young's modulus (N/mm^2)	Average pull off forces (mN)
3	D0B0	9.04E-2 ±2.05E-5	9.51E-2±4.4E-3	-1.42±2.48E-4
9	D0B0	8.25E-2±6.25E-6	9.37E-2±1.85E-3	-0.85±2.44E-4
3	D2.5B0	5.42E-2±2.00E-5	1.35E-1±0	-2.10±7.09E-4
9	D2.5B0	1.90E-1±1.28E-4	1.27E-1±4.67E-3	-1.50±8.01E-4
3	D5B0	1.54E-1±3.14E-5	1.14E-1±2.96E-3	-3.31±2.62E-4
9	D5B0	6.23E-2±7.06E-6	1.10E-1±9.32E-3	-1.11±3.06E-4
3	D10B0	1.64E-1±5.80E-7	1.89E-1±1.25E-2	-5.89±4.54E-4
9	D10B0	6.40E-2±1.07E-5	1.94E-1±1.52E-3	-1.60±6.65E-4
3	D0B2.5	1.40E-1±7.20E-5	1.53E-1±1.26E-3	-4.39±1.20E-3
9	D0B2.5	5.99E-2±1.74E-5	1.46E-1±0	-1.04±3.39E-4
3	D0B10	2.5E-1±2.65E-5	1.55E-1±3.03E-3	-6.56±4.60E-4
9	D0B10	1.05E-1±1.82E-5	1.46E-1±7.39E-3	-4.09±3.84E-4
3	D2.5B10	5.9E-1±0E+0	1.52E-1±0E+0	-14±2.12E-3
9	D2.5B10	1.07E-1±1.28E-1	1.28E-1±6.62E-3	-2.85±1.21E-3
3	D5B10	4.04E-1±2.24E-4	1.32E-1±1.54E-2	-7.69±3.90E-3
9	D5B10	2.58E-1±2.32E-4	1.09E-1±4.29E-3	-0.44±7.90E-5
3	D10B10	3.8E-1±2.00E-5	1.74E-1±4.26E-3	-10.5±3.16E-3
9	D10B10	1.08E-1±6.64E-6	1.55E-1±1.78E-2	-1.11±2.00E-5
3	D10B2.5	4.71E-1±1.53E-4	1.38E-1±8.17E-3	-10.5±3.16E-3
9	D10B2.5	6.11E-2±1.50E-5	1.43E-1±8.32E-3	-0.93±2.51E-4

When control hydrogels D0B2.5 and D0B10 were analyzed, work of adhesion values of $1.4E-1 \pm 7.20E-5 mJ/m^2$ and $2.5E-1 \pm 2.65E-5 mJ/m^2$ were obtained.

Additionally, the maximum pull off forces showed an increasing trend from $-4.39 \pm 1.20E-3mN$ to $-6.56 \pm 4.60E-4mN$ when the AAPBA content was increased from 2.5 to 10 mol% as can be seen in figure 4.15. At pH 9, the average work of adhesion

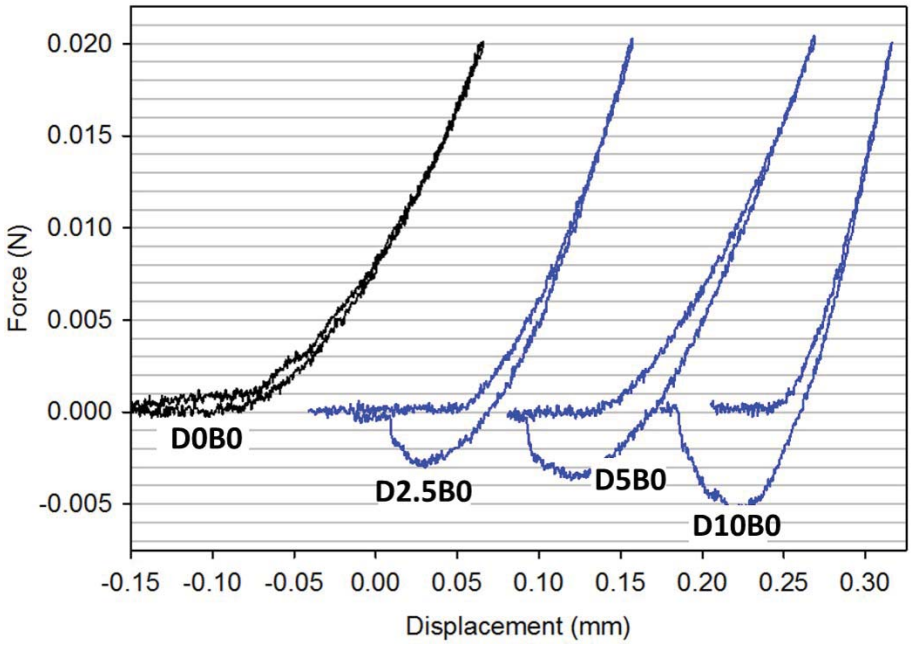

Figure 4.14: The figure is a representation of the force versus displacement curves obtained from the first contact of the control hemispherical hydrogels with increasing amounts of DMA introduced into the HEAA backbone, with a glass surface in conjunction with $250\mu L$ of a buffered medium at pH 3.

for the D0B0 was $8.25E-2 \pm 6.25E-6 mJ/m^2$. On adding increasing quantities of DMA to the network, the values observed were $1.9E-1 \pm 1.28E-4 mJ/m^2$ and $6.4E-2 \pm 1.07E-5 mJ/m^2$ for D2.5B0 and D10B0 respectively. The pull off forces registered were $-1.5 \pm 8.01E-4 mN$ and $-1.6 \pm 6.64E-4 mN$ for the same compositions. See figure 4.16.

For the control set of hydrogels D0B2.5 and D0B10, the maximum pull off forces were $-1.04 \pm 3.39E-4 mN$ and $-4.09 \pm 3.84E-4 mN$ respectively, see figure 4.17. The works of adhesion for the same set were $5.99E-2 \pm 1.74E-5 mJ/m^2$ and $1.05E-1 \pm 1.82E-5 mJ/m^2$ respectively.

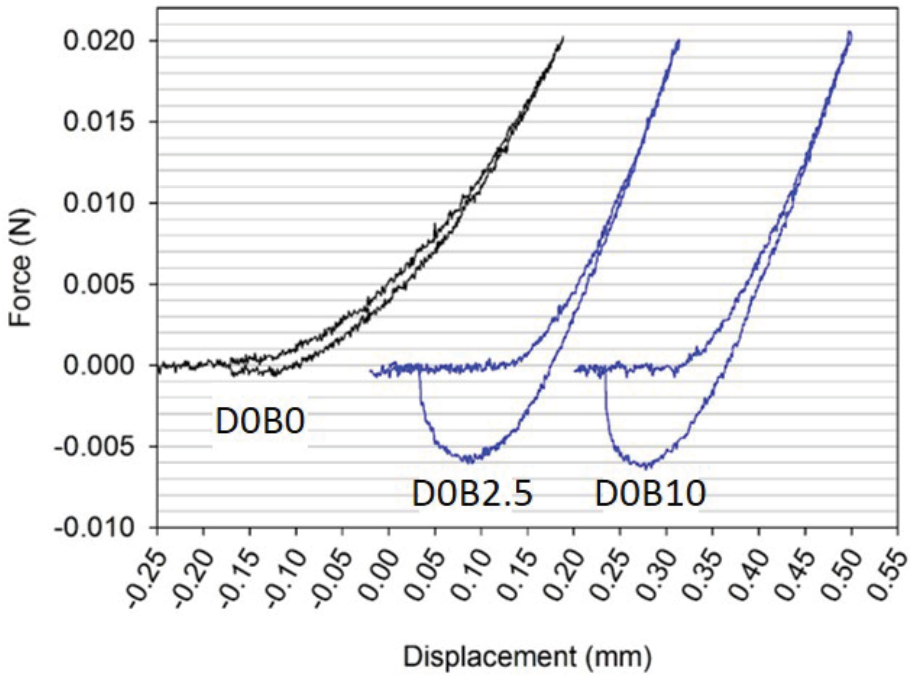

Figure 4.15: Force versus displacement curves for hydrogels containing increasing amounts of AAPBA in the polymer matrix, obtained from the first contact of hemispherical hydrogels with a glass surface in conjunction with $250\mu L$of a buffered medium at pH 3

In order to test the adhesion capabilities of the hydrogels consisting of the adhesive moiety, DMA and the protecting group, AAPBA, hydrogels with varying compositions of DMA and AAPBA co-existing with the HEAA backbone were examined for maximum pull off forces and work of adhesion values, see figure 4.18.

For D2.5B10, the work of adhesion is 5.19E-1mJ/m^2 which is greater than the values observed for each of the individual components that were a part of the hydrogel network.

Also, the maximum pull off forces observed for this testing set is 14 mN, which is considerably higher than those recorded for each of the independent moieties and the

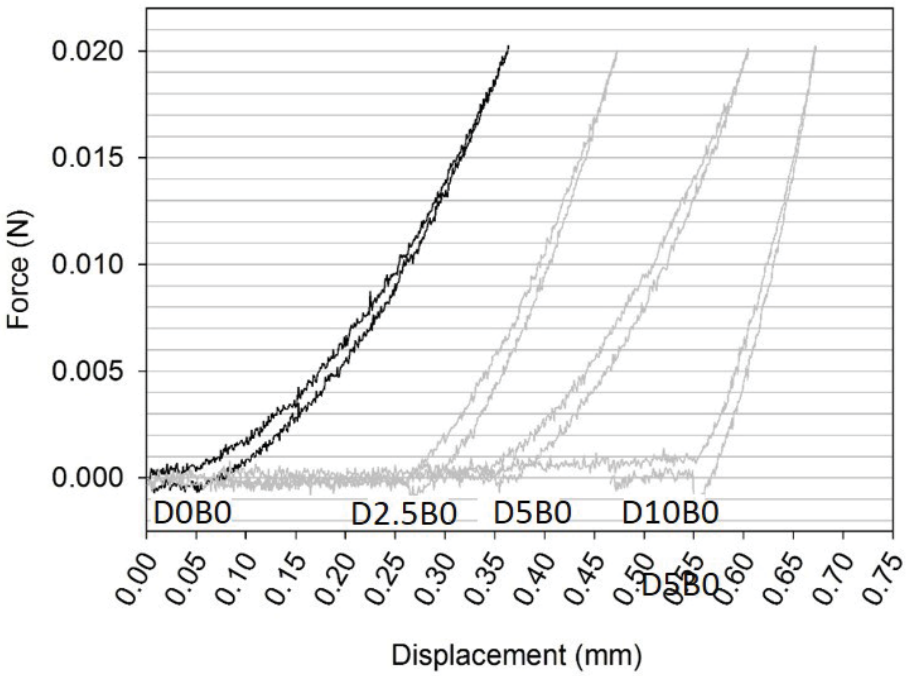

Figure 4.16: Force versus displacement curves for hydrogels containing increasing amounts of DMA in the polymer matrix, obtained from the first contact of hemispherical hydrogels with a glass surface in conjunction with $250\mu L$ of a buffered medium at pH 9

other testing set of hydrogels; figure4.18. Other testing sets of hydrogels, see table 4.2 consisting of different ratios of DMA and AAPBA co-existing in the hydrogel adhesive, also exhibited increased works if adhesion when compared to the controls embedded with the moieties individually. For example, the adhesive interaction of gel D10B2.5 amounted to 4.71E-4J/m^2 and the maximum pull off force was 1.05E-2 N, see table 4.2. The testing set of hydrogel D10B10 displayed an average work of adhesion of $3.8E-1 \pm 2E-5mJ/m^2$ and an average maximum pull off force of $-10.5 \pm 3.16E-3mN$. D5B10 showed a work of adhesion of $4.04E-1 \pm 2.24E-4mJ/m^2$ and an average maximum pull off force of $-7.69 \pm 3.9E-3mN$.

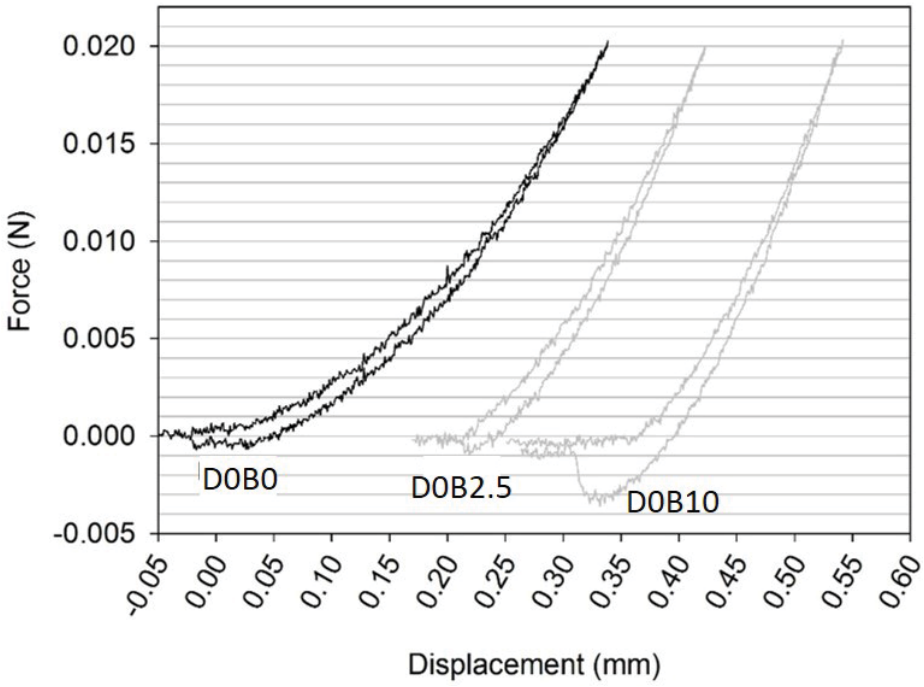

Figure 4.17: Force versus displacement curves for hydrogels containing increasing amounts of AAPBA in the polymer matrix, obtained from the first contact of hemispherical hydrogels with a glass surface in conjunction with $250\mu L$ of a buffered medium at pH 9

To compare the strengths of adhesion at acidic and basic pHs, the same set of control hydrogels were tested at acidic and basic pHs for their works of adhesion, maximum pull off forces and and Young′s moduli. The testing set of hydrogels that demonstrated the maximum work of adhesion (D2.5B10 at pH 3) show a reduced work of adhesion of $1.07E-1 \pm 1.28E-1 mJ/m^2$ for D2.5B10 at pH 9.

Also, the maximum pull off value is reduced considerably to -2.85E-3 N 4.19. For D10B2.5 at pH 9, the work of adhesion is 6.11E-5 J/m^2, and the maximum pull off force is -9.27E-4 N. D10B10 at pH 9 demonstrates a work of adhesion of 1.08E-4 J/m^2 and a maximum pull off force of -1.11E-3 N while D5B10 at the same pH shows a

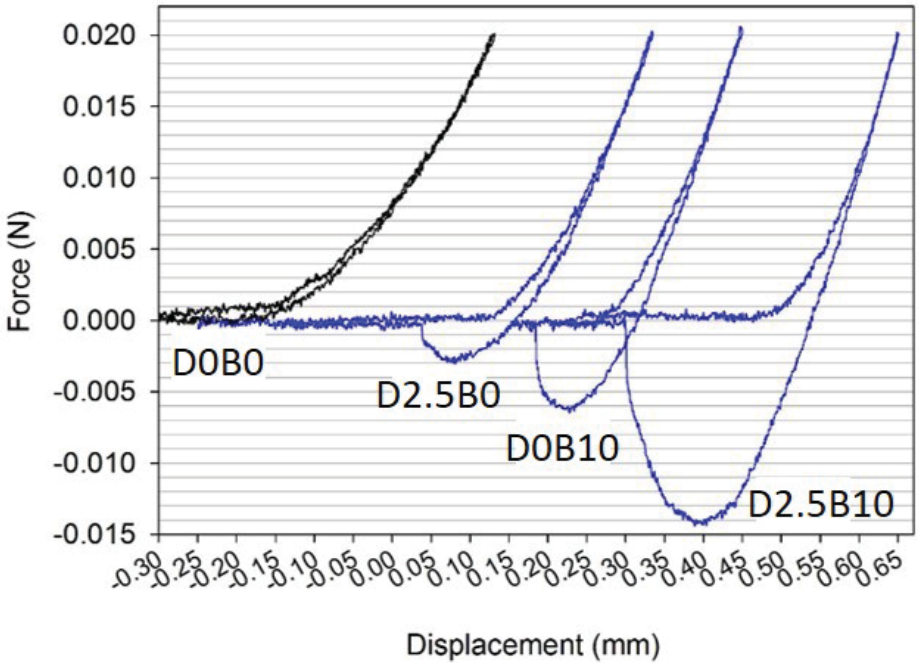

Figure 4.18: The figure is comparative representation of the force versus displacement curves for the testing sample D2.5B10 at pH 3 and its constituent elements, D2.5B0 and D0B10 at pH 3. It can be seen that D2.5B10 shows an elevated pull-off force (negative direction of Y-axis) in relation to the controls, D2.5B0 and D0B10.

work of adhesion and pull off forces of 2.58E-4 N and 4.42E-4 N respectively.

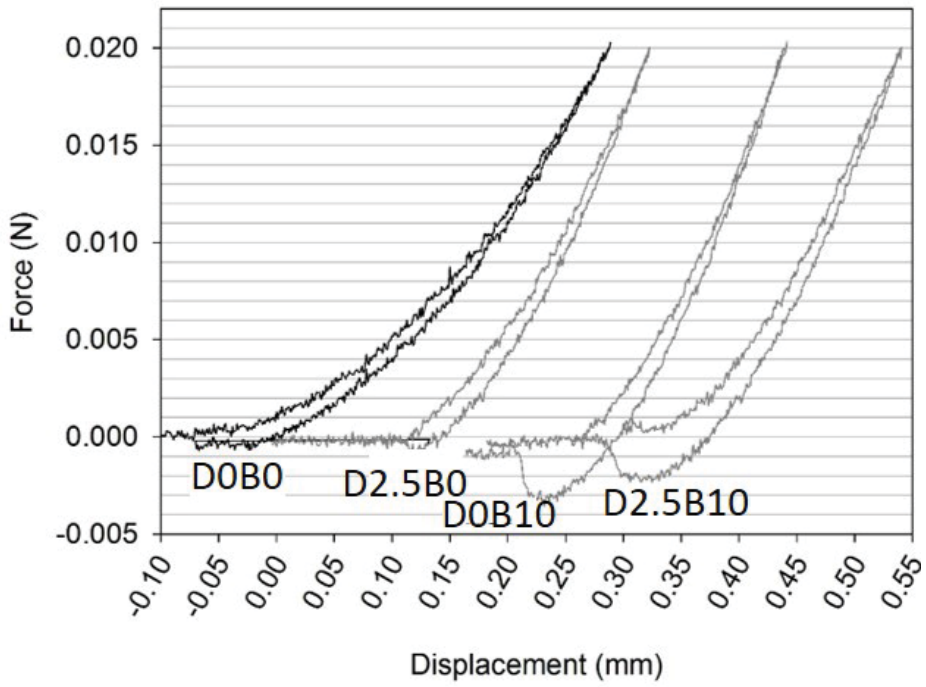

Figure 4.19: This graph is a comparative representation of the force versus displacement curves for D2.5B10 at pH 9 and its constituent elements, D2.5B0 and D0B10.

Discussion regarding the work of adhesion, Young′s modulus

As a neutral polymer backbone, N- HEAA was not expected to adhesively bind to the borosilicate glass surface; thus providing an effective means to gauge the response of the introduction of the adhesive moiety, DMA and the protecting group, AAPBA into the polymer network. At pHs 3 and 9, the D0B0 control hydrogels did not exhibit any adhesive interaction with the surface. The work of adhesion values at pH 3 and pH 9 were $9.04E-2 \pm 2.05E-5 mJ/m^2$ and $8.25E-2 \pm 6.25E-6 mJ/m^2$. The average values of Young′s moduli were comparable at $9.51E-2 \pm 4.4E-3 N/mm^2$ at pH 3 and $9.37E-21.85E-3 N/mm^2$ at pH 9. There was no hysteresis between the loading and unloading cycles, confirming the absence of any adhesive moiety in the hydrogel. Also, no forces were recorded in the negative Y-direction. When increasing amounts of DMA were added to D0B0, for the gels immersed in a pH 3 buffered solution for 48 hours and tested as shown in the illustration, there was a corresponding increase in the values of work of adhesion. The maximum work of adhesion was observed for D10B0. Additionally, the area encapsulated by the curve is the highest for D10B0 in pH 3. There was a 3 fold increase in the values as compared to D2.5B0. Also, the maximum pull- off forces recorded for the D10B0 control hydrogels is 2.8 times higher than those for 2.5 mol% DMA. It can hence be concluded that elevating the mol% of DMA in the polymer network increases the presence of the catecholic groups that are responsible for surface adhesion, figure 4.20. The Young′s moduli in both cases is comparable, with the 10 mol% DMA being slightly stiffer ($1.89E-1 \pm 1.25E-2 N/mm^2$) than

the 2.5mol%DMA ($1.35E-1 \pm 0.00N/mm^2$). These values are higher than those observed for D0B0 at pH 3. This is perhaps because addition of increasing amounts of DMA translates into higher crosslinking between the DMA and HEAA, making the gels stiffer. Although at pH 9, the work of adhesion for the hydrogel D2.5B0 was found to be slightly higher than that at pH 3, the work of adhesion for the control groups containing D5B0 and D10B0 reduced considerably at pH 9 as compared to the values at pH 3. Also, because the average maximum pull off forces for the hydrogel adhesives at pH 3 were considerably higher than that at pH 9, the deviation from normal trend for decreasing work of adhesion values can be ignored. It has been documented that the oxidation of the catecholic groups at pH values above the pK_a of catechol results in the formation of benzoquinone [7] [34] [9]. This phenomenon is expected to be a deterrent to substrate binding capabilities of catechol[4] [8]. It should be noted that at pH 9, there was no significant difference between the works of adhesion for control hydrogels D2.5B0, D5B0 and D10B0, indicating that the catecholic groups were completely oxidized in the time period of 48 hours that they were immersed in pH 9 TRIS buffered solutions. Interestingly, at pHs 3 and 9, the control set of hydrogels D0B2.5 and D0B10, exhibited adhesive interaction with the glass substrate. The values of work of adhesion for D0B2.5 and D0B10 at pH 3 not show any striking difference. However, at pH 9, the average work of adhesion value was higher (1.75 times) for D0B10 as compared to the D0B2.5 samples. The Young′s moduli for both these compositions is comparable at corresponding acidic

and basic pHs. Although the presence of AAPBA in a hydrogel network has not been documented to enhance the adhesive properties of the hydrogels, there is a likelihood of the trigonal/tetrahedral moiety interacts with the traces of Boron atoms in the borosilicate glass which is used as the substrate which could be seen from the average maximum pull off forces observed especially at pH 3. Further investigation is required to fully understand the nature of the interaction of AAPBA with the glass substrate at acidic and basic pHs.

Controls with combination pH 3 and pH 9

At pH 3, D2.5B10 exhibited an elevated work of adhesion ($5.9E-1 \pm 0.00 mJ/m^2$) as compared to the individual elements in the polymer matrix. From the table 4.2, it can be concluded from the Young′s moduli, that these hydrogels were also stiffer as compared to the HEAA backbone, but had comparable moduli with respect to the D2.5B0 and D0B10 at pH 3. This indicates that the polymerization of the DMA and AAPBA with the polymer network has the same effect on the Young′s modulus independently as well as when both elements co-exist. This information can also be used to infer that there isnt any additional crosslinking between the DMA and the AAPBA within the hydrogel adhesive. Additionally, there is a significant increase in the maximum pull- off forces observed for this combination of DMA and AAPBA. If the individual components are taken into account, D0B10 demonstrates an average maximum pull off force of $-6.56 \pm 4.60 mN$ and D2.5B0 exhibits $-2.1 \pm 7.09E-4 mN$,

while the D2.5B10 results in a maximum pull off force of $-14 \pm 2.12mN$, which is a more than a twofold increase when compared to the higher of the two individual pull off forces. This is because of the fact that the catecholic functional groups that impart the adhesive properties to the hydrogel bind to the substrate in the presence of an acidic pH environment via H-bonds [8] [6] as can be seen in the representative figure 4.20.

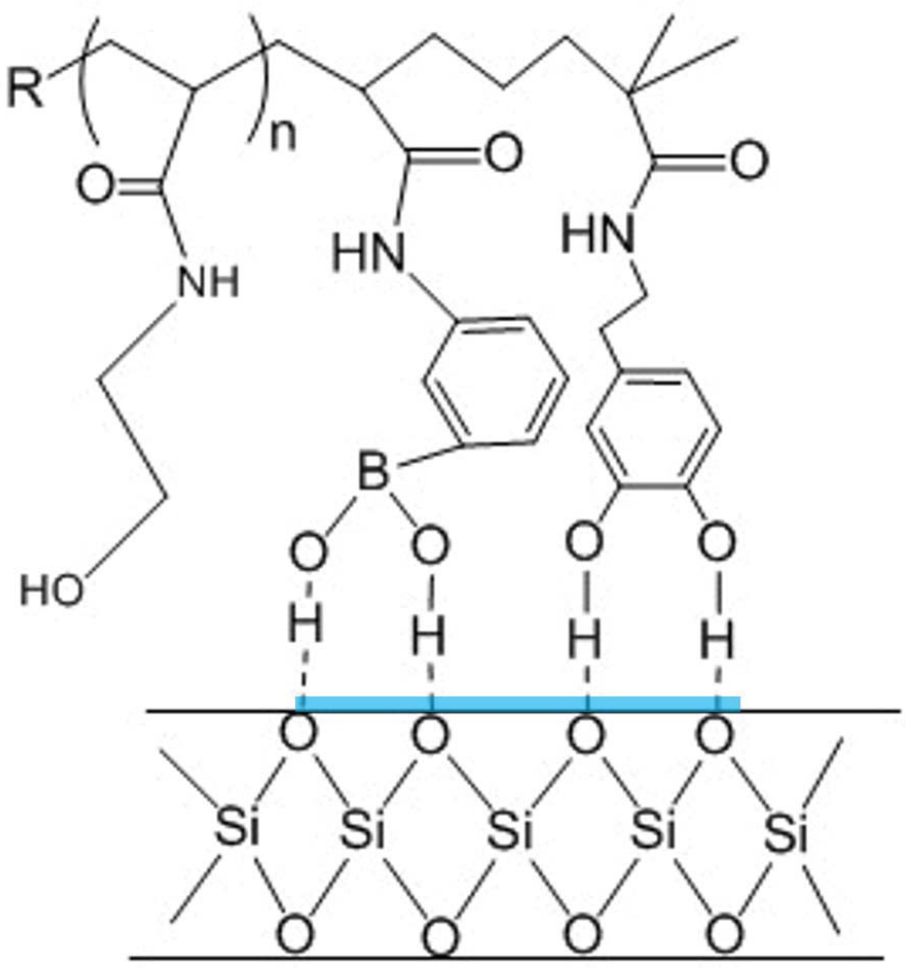

Figure 4.20: Adhesive interaction of the hydrogel to the borosilicate glass surface

This, in addition to the unusual adhesive interaction of the AAPBA at pH 3 with the

substrate is most likely responsible for enhanced adhesive interaction. At pH 9, the work of adhesion values for D2.5B10 composition reduces 4.85 times in comparison to the values observed at pH 3. This is because at pH 9, the catecholic groups form a coordinate complex with the PBA groups and the resulting complexation essentially means that the catecholic groups will no longer be available for interfacial binding with the glass substrate; see figure 4.21.

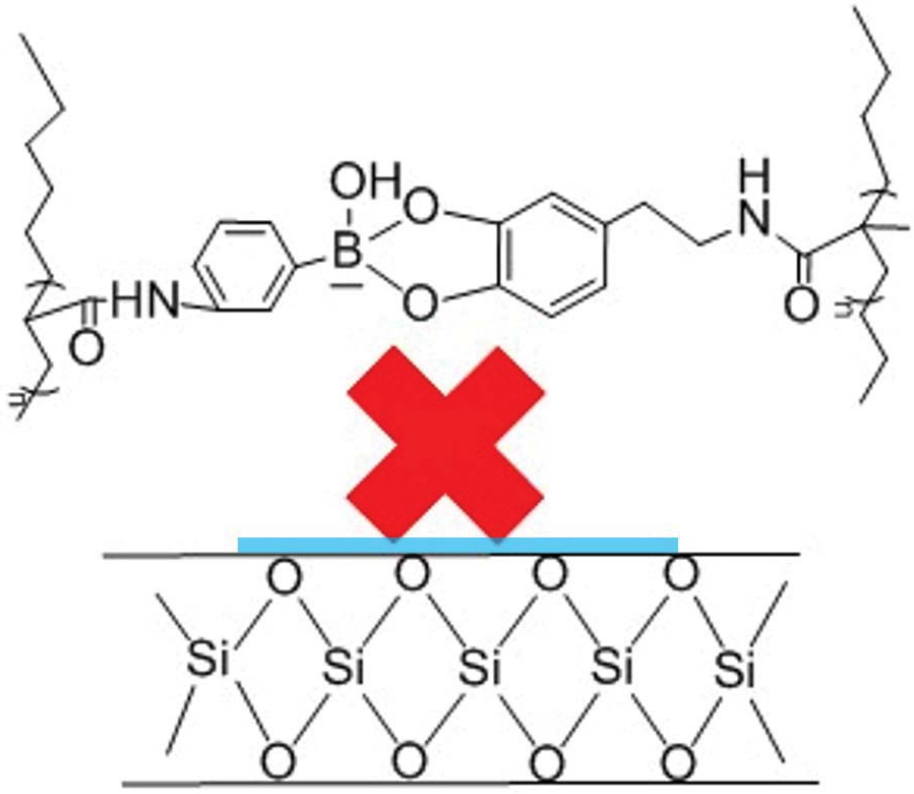

Figure 4.21: No interaction once the complex is formed

Although there is no remarkable difference in the Young′s moduli at the two pHs, there is also a striking lowering of the maximum pull- off force, which was determined to be $-2.85 \pm 1.21E - 3mN$ (almost a 5 fold decrease). In spite of the reduction

in the maximum pull- off forces, it must be noted that the adhesive interaction does not diminish to zero. Although it was expected that presence of excessive amounts of AAPBA in comparison to the DMA should ensure the complete complexation of catecholic groups with the PBA functionality, the results from the contact mechanics test indicated that either some DMA was still left uncomplexed. Photographic evidence of the hydrogel discs, 15 mm in diameter and 2mm in thickness indicated a very light brownish tinge (catechol on oxidation turns brown) after immersion in pH 9 for 48 hours; refer to figure B.7,supporting information in [29]. This, in comparison to the same composition and morphology immersed in pH 3 indicated a clear, transparent hydrogel. This gives us further reason to believe that there exists some uncomplexed DMA at pH 9. Also, because the control hydrogel D0B10 demonstrated an average maximum pull off force of $-6.56 \pm 4.60E-4mN$ at pH 3, the interaction of the uncomplexed AAPBA with the borosilicate glass needs to be studied in detail in the future. For the other combinations tested at pHs 3 and 9, viz. D10B10, D5B10 and D10B2.5, the Young′s moduli were comparable. Wetting is largely considered one of the major constraints for strong adhesive performance of an adhesive. In this study, we have been able to demonstrate wet adhesion, using a series of experiments on our hydrogel adhesives that are more physiologically pertinent. According to Lee et al. [8] such kind of a testing mechanism can help to exclude certain interactions like Van der Waals′ interactions etc. which makes it more significant, albeit difficult to perform. A thorough study of the relation between the increasing amounts of DMA and

its effect on the adhesive capabilities of the hydrogel needs to be conducted. Also, to better understand the protective role of AAPBA needs to be looked at with more appropriate analytical techniques.

Discussing about different compositions being effective for different applications

From the contact mechanics tests, it was observed that different compositions exhibited varying levels of interfacial binding with the borosilicate glass surface. Some of the compositions tested exhibited the same order of magnitude of work of adhesion values at both- acidic and basic pHs. On the other hand, certain ratios of DMA and AAPBA yielded results that showed a higher adhesion at acidic pH as compared to basic pHs. For example, D5B10 displayed average work of adhesion values that were of the same order of magnitude in pH 3 as well as in pH 9. However,D10B10, D5B10 and D2.5B10 showed higher average work of adhesion at acidic pHs when compared to the basic pHs.

4.6 Reversibility studies

In the reversibility swelling studies, the swelling behavior of the controls was compared with the swelling behavior of the testing set of hydrogels. By comparing the values

of the diameters of the hydrogels that were transferred into pH 3 after 48 hours of immersion in pH 9 solution to those of the original pH 3 samples, a relation was established between the ability of the polymer to recover its original diameter upon the switching of pH from a basic to an acidic value.

4.6.1 Swelling studies results

In order to determine the ability of the hydrogels to reversibly shrink and swell in acidic and basic mediums respectively, a basic swelling study was performed. The diameters of the hydrogel equilibrated in the pH buffered solutions was recorded at fixed time intervals using a pair of digital vernier callipers. While doing so, the change of pH from basic to acidic was carried out to deduce the effect of pH on the diameter of the hydrogels. From the swelling tests, it was observed that all the combinations of gels tested were swollen to a lesser extent in acidic pH as compared to the same set immersed in basic pH. While immersed in the acidic pH, the catechol and the boronic acid groups do not interact with each other (after a time lapse). The gels were removed from the acidic medium and washed ith DI water to ensure that no unreacted monomers remained on the surface. On immersion into pH9, the control gels containing varying proportions of DMA are expected to get oxidized (after a time lapse)while the testing set of hydrogels that contain a combination of DMA and AAPBA is expected to form 'reversible' bonds by means of catechol-boronic acid

complexation. This bond allows for the protection of the adhesive groups of DMA. When these hydrogels are transferred into acidic pH, the complexation should not longer exist (after a time lapse) because the pH is significantly lower than the pK_a required for the formation of the complex. (time lapse= 48 hours)

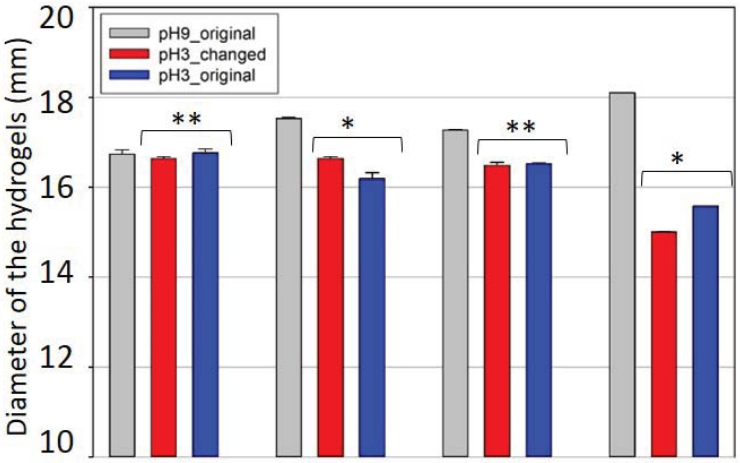

DMA(mol%)	0	10	0	10
AAPBA(mol%)	0	0	2.5	2.5

Figure 4.22: Reversibility of the catechol-boronic acid complex for hydrogel D10B2.5 measured in terms of their diameter and in relation with the controls: D0B0, D10B0, D0B2.5. *p $<$ 0.05, **p $>$ 0.05

For hydrogels consisting of 10mol%DMA and 2.5mol% AAPBA, the average diameter of the hydrogels immersed in pH 9 for 48 hours was $18.1 \pm 0.00mm$. This set of 3 samples was rinsed with DI water, transferred into a pH 3 buffered solution and allowed to nutate for another 48 hours. At the end of 48 hours, the diameter of the hydrogels was found to be $15.01 \pm 9.43E{-}3mm$ which was comparable to the hydrogels immersed in pH 3 and nutated for 48 hours ($15.58 \pm E0.00mm$). HEAA being a neutral backbone did not exhibit any significant change in diameter in response to the

changing pH values; See figure 4.22. The other controls in this experiment displayed a similar trend in which the diameters of the hydrogels after changing the environment (from pH 9 to pH 3) were in the same range as the samples that were immersed in pH 3. However, the change in the diameter was maximum for the hydrogels containing both the elements viz. DMA and AAPBA in the hydrogel. When hydrogels consisting of 10mol%DMA and 10mol%AAPBA were examined after 48 hours, the hydrogels that had swelled to an average of $22.24 \pm 0.02mm$ in pH 9, later shrunk to an average of $13.5 \pm 4.71E-3mm$ after being transferred to pH 3 and allowed to equilibrate for 48 hours. This again was comparable to the average diameter ($14.65 \pm 0.04mm$) of hydrogels that were originally immersed in pH 3 for 48 hours. The results obtained from the other testing sets of hydrogels also revealed that the diameters show a tendency to return to a value within the the range comparable to hydrogels that were immersed in pH 3 for 48 hours.

4.6.2 Rheological analyses

The samples were tested according to the same protocol that was employed for the previous rheometry tests. The loss and storage moduli obtained from the frequency sweep were analyzed. The rheological data was compared with that of the samples that were originally immersed in pH 3 solution for 48 hours. The general trend showed that neither the storage nor the loss modulus of the hydrogels could return to the

exact moduli represented by the original pH 3 hydrogels, see figure 4.23. However, there is less than an order of magnitude of difference between the storage moduli of the original versus the changed pH samples, see figure4.24. For D10B2.5 at pH 3, the difference was the least.

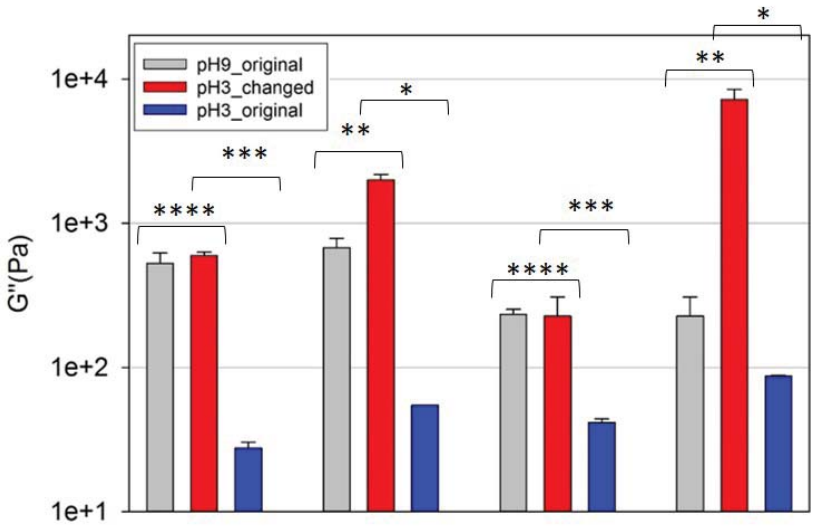

DMA(mol%)	2.5	5	10	10
AAPBA(mol%)	10	10	2.5	10

Figure 4.23: The effect of changing pH on G". ****p > 0.05, *p, **p < 0.05, ***p = 0.05.

This could be likely because D10B2.5 was composed of the lowest amount of AAPBA in relation to the DMA as a part of the hydrogel matrix. The lower degree of complexation could mean that it was easier for the polymer to regain its chemical and hence, mechanical structure at pH 3. Although it is difficult to predict the exact microstructural properties of this new set of hydrogel adhesives, the qualitative and quantitative data from the swelling tests indicates that the macrostructure of the samples shows close relation to the original pH 3 samples in terms of its diameter.

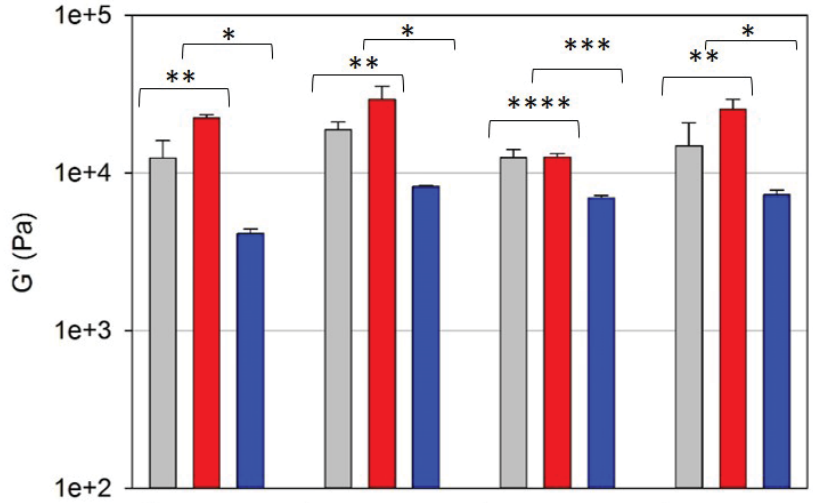

DMA(mol%)	2.5	5	10	10
AAPBA(mol%)	10	10	2.5	10

Figure 4.24: The effect of changing pH on G′. *p, **p < 0.05 , ***p $= 0.05$, ****p > 0.05

4.6.3 Lack of enough evidence to prove reversibility using swelling and rheometry

It must be noted that the hydrogels that were transferred from pH 9 to pH 3 after 48 hours and then equilibrated in pH 3 for another 48 hours were effectively influenced by an aqueous medium for 96 hours. During the first phase of its immersion in pH 9, the complexation caused the hydrogel to swell. When these samples were rinsed and introduced into the pH 3 buffered solution, it is very likely that it is difficult for the H^+ions to first, penetrate into the hydrogel matrix and second, provide for the breaking of the coordination complex. We believe that lowering the pH further could

make more H^+ ions available for the effective de-coupling. Also, due to the absence of an effective control for this extended time period of immersion, the comparison of the properties of this essentially new set of hydrogels to those of the hydrogels immersed in either of the acidic or basic solutions for 48 hours does not do complete justification.

Chapter 5

Summary

Prior studies have demonstrated that the addition of DMA, a synthetic form of mussel adhesive protein, enhances the adhesive interaction between the synthesized adhesive and a wide array of organic and inorganic substrates under different conditions. Research in this direction has not been able to generate substantial evidence at a macromolecular level [46]. Additionally, there still isn′t a clear understanding of the molecular- level interaction of the catecholic groups that bind to chemically varying substrates [47]. We have succeeded in copolymerizing DMA with HEAA and have also been able to introduce AAPBA in the polymer network to preserve the adhesive capabilities of the catecholic groups by forming the reversible catechol- boronic acid complex as a stimulus to an external pH trigger. It would mean that extreme conditions like elevated temperatures [12] would no longer be needed in order to separate

delicate bodily components like soft tissues, organs, etc. and the complexation could be used to promote debonding triggered by a relatively simple change in pH values. Although there are certain properties like ideal complexation stoichiometry and reversibility that need added proof, we believe this is a novel model adhesive system that could be employed in multiple fields besides biomedical engineering.

Chapter 6

Conclusion

Rheological data shows that while the synthesized hydrogel adhesives containing DMA and AAPBA in addition to the N-HEAA backbone behave as covalently cross linked- elastic hydrogels at pH 3, at pH 9, the introduction of AAPBA leads to formation of additional physical coordinate crosslinks. The analysis of the swelling characteristics of the hydrogels revealed that the formation of the catechol- boronic acid complex, that leaves a negative charge on the Boron atom results in a greater magnitude of swelling for the hydrogels at a basic pH. Although the formation of the complex increases the G' values, it does not quite translate into a reduced swelling phenomenon. This could be likely because of the dominant repulsion of the polymer network in basic pH in comparison with the statistically insignificant increase in G' as a result of the complex. At pH 9, the breaking of the reversible bonds

transformed into elevated G'' values. Contact mechanics data displayed evidence regarding the ability of the DMA containing hydrogels to adhesively interact with an inorganic(borosilicate glass) surface under wet conditions. When hydrogel adhesives containing DMA and AAPBA were tested, the works of adhesion were found to be higher than the control sets that were tested at pH 3. Moreover, the adhesion of the control sets was greatly reduced at pH 9. Due to the presence of AAPBA in the polymer network, it is expected that the reduced adhesion is a result of the complexation and not the complete oxidation of catechol to orthoquinone. In spite of the fact that qualitative evidence from pictures taken of the hydrogels immersed in pH 9, see figure B.7 visually indicated that hydrogels containing a combination of DMA and AAPBA were not completely oxidized as compared to the DMA controls, and due to the unexpected adhesive interaction exhibited by AAPBA at both these pHs, a more detailed testing is needed to conclusively determine the chemistry of interaction.

Chapter 7

Future work

We have demonstrated a model contact mechanics setup experiment to determine the interfacial binding capabilities of DMA containing hydrogel with AAPBA as the adhesion protecting group. We propose using electrochemical oxidation as a means of controlling the redox catechol chemistry, which could ultimately result in the design of electic current responsive adhesives i.e using electro-osmosis to control the bonding-debonding mechanism. This would enable us to have a more controlled redox scheme for catechol, meaning quicker actuation and simpler means of controlling the environmental cues. Also, an array of microfibrillar structures (using microfabrication) could be employed to increase the adhesion capabilities by means of increasing the available surface area. In addition to this, the introduction of a high resolution camera into the contact mechanics setup for imaging the changes in the microstructure would give us

a deeper insight into the interfacial binding properties of the hydrogel.

References

[1] Qin, Z.; Buehler, M. J. *Nature communications* **2013**, *4*.

[2] Lee, B. P.; Messersmith, P.; Israelachvili, J.; Waite, J. *Annual Review of Materials Research* **2011**, *41*(1), 99–132.

[3] Yu, J.; Wei, W.; Menyo, M. S.; Masic, A.; Waite, J. H.; Israelachvili, J. N. *Biomacromolecules* **2013**, *14*(4), 1072–1077.

[4] Lee, H.; Scherer, N. F.; Messersmith, P. B. *Proceedings of the National Academy of Sciences* **2006**, *103*(35), 12999–13003.

[5] Kan, Y.; Danner, E. W.; Israelachvili, J. N.; Chen, Y.; Waite, J. H. 10 **2014**, *9*(10), e108869.

[6] Hwang, D. S.; Harrington, M. J.; Lu, Q.; Masic, A.; Zeng, H.; Waite, J. H. *J. Mater. Chem.* **2012**, *22*, 15530–15533.

[7] Wheeler, D. E.; Rodriguez, J. H.; McCusker, J. K. *The Journal of Physical Chemistry A* **1999**, *103*(20), 4101–4112.

[8] Lee, B. P.; Chao, C.-Y.; Nunalee, F. N.; Motan, E.; Shull, K. R.; Messersmith, P. B. *Macromolecules* **2006**, *39*(5), 1740–1748.

[9] Spyroudis, S. *Molecules* **2000**, *5*(12), 1291–1330.

[10] Ye, Q.; Zhou, F.; Liu, W. *Chem. Soc. Rev.* **2011**, *40*, 4244–4258.

[11] Heinzmann, C.; Coulibaly, S.; Roulin, A.; Fiore, G. L.; Weder, C. *ACS Applied Materials & Interfaces* **2014**, *6*(7), 4713–4719.

[12] Luo, X.; Lauber, K. E.; Mather, P. T. *Polymer* **2010**, *51*(5), 1169 – 1175.

[13] White, E. M.; Seppala, J. E.; Rushworth, P. M.; Ritchie, B. W.; Sharma, S.; Locklin, J. *Macromolecules* **2013**, *46*(22), 8882–8887.

[14] Banea, M.; da Silva, L.; Campilho, R. *The Annals of Dunarea de Jos University of Galati Fascicle XII, Welding Equipment and Technology* **2013**, *24*, 11–14.

[15] Hwang, D. S.; Harrington, M. J.; Lu, Q.; Masic, A.; Zeng, H.; Waite, J. H. *Journal of materials chemistry* **2012**, *22*(31), 15530–15533.

[16] Ye, Q.; Zhou, F.; Liu, W. *Chemical Society Reviews* **2011**, *40*(7), 4244–4258.

[17] Guvendiren, M.; Messersmith, P. B.; Shull, K. R. *Biomacromolecules* **2007**, *9*(1), 122–128.

[18] Yu, M.; Hwang, J.; Deming, T. J. *Journal of the American Chemical Society* **1999**, *121*(24), 5825–5826.

[19] Cambre, J. N.; Sumerlin, B. S. *Polymer* **2011**, *52*(21), 4631–4643.

[20] Lim, H. L.; Hwang, Y.; Kar, M.; Varghese, S. *Biomaterials Science* **2014**, *2*(5), 603–618.

[21] Omidian, H.; Hasherni, S.-A.; Askari, F.; Nafisi, S. *Iranian J. of Polymer Science and Technology Vol* **1994**, *3*(2).

[22] Lee, H.; Lee, B. P.; Messersmith, P. B. *Nature* **2007**, *448*(7151), 338–341.

[23] Lee, B. P.; Konst, S. *Advanced Materials* **2014**, *26*(21), 3415–3419.

[24] Fischer-Cripps, A. C.; Mustafaev, I. *Introduction to contact mechanics;* Springer, 2000.

[25] Mian, S. A.; Gao, X.; Nagase, S.; Jang, J. *Theoretical Chemistry Accounts* **2011**, *130*(2-3), 333–339.

[26] Hertz, H. *Angew. Math* **1881**, *92*, 156–171.

[27] Shull, K. R.; Chen, W.-L. *Interface Science* **2000**, *8*(1), 95–110.

[28] Flanigan, C. M.; Crosby, A. J.; Shull, K. R. *Macromolecules* **1999**, *32*(21), 7251–7262.

[29] He, L.; Fullenkamp, D. E.; Rivera, J. G.; Messersmith, P. B. *Chemical Communications* **2011**, *47*(26), 7497–7499.

[30] Yan, J.; Springsteen, G.; Deeter, S.; Wang, B. *Tetrahedron* **2004**, *60*(49), 11205–11209.

[31] Springsteen, G.; Wang, B. *Tetrahedron* **2002**, *58*(26), 5291–5300.

[32] Bull, S. D.; Davidson, M. G.; Van den Elsen, J. M.; Fossey, J. S.; Jenkins, A. T. A.; Jiang, Y.-B.; Kubo, Y.; Marken, F.; Sakurai, K.; Zhao, J.; others. *Accounts of chemical research* **2012**, *46*(2), 312–326.

[33] Chen, G. C.; others. *Wood and Fiber science* **2008**, *40*(2), 248–257.

[34] Guin, P. S.; Das, S.; Mandal, P. *International Journal of Electrochemistry* **2011**, *2011*.

[35] Kim, A.; Mujumdar, S. K.; Siegel, R. A. *Chemosensors* **2013**, *2*(1), 1–12.

[36] Skelton, S.; Bostwick, M.; O'Connor, K.; Konst, S.; Casey, S.; Lee, B. P. *Soft Matter* **2013**, *9*(14), 3825–3833.

[37] Pappin, B.; Kiefel, M. J.; Houston, T. A. *Boron-Carbohydrate Interactions;* INTECH Open Access Publisher, 2012.

[38] Pizer, R.; Babcock, L. *Inorganic Chemistry* **1977**, *16*(7), 1677–1681.

[39] Hoffman, A. S. *Advanced drug delivery reviews* **2012**, *64*, 18–23.

[40] Contact mechanics, 1985. Johnson, K. **1974**.

[41] Chung, H.; Glass, P.; Pothen, J. M.; Sitti, M.; Washburn, N. R. *Biomacromolecules* **2010**, *12*(2), 342–347.

[42] Flanigan, C. M.; Shull, K. R. *Langmuir* **1999**, *15*(15), 4966–4974.

[43] Robitaille, M.; Shi, J.; Wan, K.-t.

[44] Shi, J.; Müftü, S.; Wan, K.-t.

[45] Arunbabu, D.; Shahsavan, H.; Zhang, W.; Zhao, B. *The Journal of Physical Chemistry B* **2012**, *117*(1), 441–449.

[46] Stepuk, A.; Halter, J. G.; Schaetz, A.; Grass, R. N.; Stark, W. J. *Chem. Commun.* **2012**, *48*(50), 6238–6240.

[47] Glass, P.; Chung, H.; Washburn, N. R.; Sitti, M. *Langmuir* **2009**, *25*(12), 6607–6612.

[48] Ding, X.; Vegesna, G. K.; Meng, H.; Winter, A.; Lee, B. P. *Macromolecular Chemistry and Physics* **2015**, *216*(10), 1109–1119.

[49] Lee, B. P.; Lin, M.-H.; Narkar, A.; Konst, S.; Wilharm, R. *Sensors and Actuators B: Chemical* **2015**, *206*, 456–462.

[50] Holten-Andersen, N.; Harrington, M. J.; Birkedal, H.; Lee, B. P.; Messersmith, P. B.; Lee, K. Y. C.; Waite, J. H. *Proceedings of the National Academy of Sciences* **2011**, *108*(7), 2651–2655.

[51] Fang, H.; Kaur, G.; Wang, B. *Journal of Fluorescence* **2004**, *14*(5), 481–489.

[52] Yamamoto, H.; Sakai, Y.; Ohkawa, K. *Biomacromolecules* **2000**, *1*(4), 543–551.

[53] Li, S.; Davis, E. N.; Huang, X.; Song, B.; Peltzman, R.; Sims, D. M.; Lin, Q.; Wang, Q. *Journal of diabetes science and technology* **2011**, *5*(5), 1060–1067.

[54] Annabi, N.; Tamayol, A.; Shin, S. R.; Ghaemmaghami, A. M.; Peppas, N. A.; Khademhosseini, A. *Nano today* **2014**, *9*(5), 574–589.

[55] Yang, J.; Stuart, M. A. C.; Kamperman, M. *Chemical Society Reviews* **2014**, *43*(24), 8271–8298.

[56] Wananuruksawong, R.; Jinawath, S.; Padipatvuthikul, P.; Wasanapiarnpong, T. In *IOP Conference Series: Materials Science and Engineering*, Vol. 18, page 192010. IOP Publishing, 2011.

[57] Araujo, P. Z.; Morando, P. J.; Blesa, M. A. *Langmuir* **2005**, *21*(8), 3470–3474.

Appendix A

Protocols for manufacture of supporting materials and addistional information

A.1 Silane coating borosilicate glass slides

Silane coating protocols and precautions

(3D-Molding of Microfluidic Devices, caltech thesis library van Dam, R. Michael (2006) Solvent-resistant elastomeric microfluidic devices and

applications. Dissertation (Ph.D.), California Institute of Technology. http://resolver.caltech.edu/CaltechETD:etd-12052005-234258) Section: Derivatization of glass for DNA synthesis

Trichloro(1H,1H,2H,2H-perfluorooctyl)silane from Sigma- Aldrich

Precautions to be taken: Corrosive to metals Skin corrosion Eye damage Flash point 870C Reacts violently with water Face Shields, full-face respirator (US), Gloves, Goggles, multi-purpose combination respirator cartridge (US), respirator filter (from Sigma-Aldrich)

Recommended procedure

1. Clean the glass slides(3x1) first with ethanol and then with distilled water 2. Dilute the silane using toluene and immerse the glass plates in the solution 3. 1 vol4. Carry out subsequent washing repeatedly using 2-3 beakers of toluene

Implementation Do not use plastic petri dishes!

1. Anhydrous toluene was used; will no longer remain anhydrous for future use 2. 0.5mL of silane was dissolved in 49mL of toluene; each side of the glass slide for 20 mins. 3. Slide immersed at 340pm. Side 2 at 4pm. Removed from solution. 4. Washed in 3 successive beakers containing Toluene for 10 minutes each. 5.Stored the slides in a dry container.

A.2 Acidic and basic pH buffer solutions

Protocol for making TRIS Tris(hydroxymethyl) aminomethane buffer

Modified TRIS buffer protocol in Lab Notebook No.2, 03042015 http://biotech.about.com/od/buffersandmedia/ht/trisbuffer.htm Tris buffer is made at pH 9 1. (mol/L)*L1 where mol/L is the molar conc of the buffer and L1 is the volume of the solution being made 2.grams of Tris base to weigh= moles* 121.4g/mol 3. Dissolve this Tris into to of the desired volume 4.Mix HCl(e.g. 1M) until the pH meter gives you the desired pH for your buffer 5. Dilute the buffer with DI water to reach the desired final volume

Implementation

Making 0.05M Tris base and 0.15M NaCl at temperature of 240C 1. Weight of Tris base measured=0.05*121.14*0.5=3.0285 2. Weight of NaCl measured=0.15*58.5*0.5=4.38 3. 400mL of DI water was added to these two chemicals present in the container 4. The pH of this solution was adjusted to 7.27 by adding 1M HCl 5.100mL of DI water was added to reach the final desired volume of 0.5L.

Acidic pH buffered mediums were made by adding appropriate quantities of 1M HCl 0.1M NaCl solution

Protocol for NaCl solution

0.1M NaCl solution was made MW of NaCl = 58.8g/mol Weight of NaCl measured =0.1*58.8*0.5=2.94g

A.3 Significance of the reacting components

HEAA

Electrically neutral, hydrophilic, non ionic The hydrophobic C-C backbone structure is masked by the presence of -OH groups As it is a monomer with an amide backbone, it does not undergo hydrolysis easily Used in adhesive formulations, coating materials, reactive diluent for UV curable resins http://www.kjchemicals.co.jp/en/product/function07.html and [53]

DMA

Dopamine methacrylamide consists of the adhesive component, DOPA directly conjugated with a polymerizable methacrylate group which enables the adhesive moiety to be incorporated into a hydrogel network configuration Hydrophobic monomer Consists of the catechol groups that can bind to a variety of substrates in a wet environment. Marine mussels use the mfps to adhere to almost any kind of substrate

viz. ceramics, metals, polymers

Inspiration from Mussel Adhesive Protein and Introduction to DMA

Mytilus edulis is a marine mussel animal that can attach itself to rocks and other foundation structures underwater by the means of byssus threads, which are composed of strong, fibrous proteins secreted in the mussels body. The marine organism secretes the liquid proteins in its foot, which enables it to form water- resistant bonds that enable it to anchor itself to almost any kind of substrate in rough, intertidal and subtidal aquatic conditions. The structure of the mussels foot consists of the following proteins: The prepolymerized collagen, viz. preCOL-D, pre COL- NG, preCOL-P-not particularly present in the distal foot but are mostly a part of the proximal proteins closer to the mussels body and are responsible for mechanical strength of the byssus. The mytilus edulis foot proteins (mefps) 2-6 are mainly responsible for adhesion. These mussel foot proteins(mfps) have different protein sequences but they all contain the amino acid, L-3,4 dihydroxyphenylalanine as a part of their sequence[2].Thus, the pre-collagens form the core of the byssus threads and the Mefps are the ones responsible for wet and dry adhesions. The mfps have been found to be abundant in L-3,4-DOPA (3,4 dihydroxyphenylalanine), which has a catecholic side chain that has been shown to bind to a variety of organic substrates like tissues, bones and inorganic metal substrates like SiO2, TiO2, Al2O3, Fe3O4, etc. under wet conditions [57], [3]. Titanium is one of the most commonly used implant materials in the biomedical

engineering field. Upon insertion in a biological environment, it quickly forms a passivation layer of TiO2. Jing Yu et *al.*[3] have demonstrated that DOPA forms a bidentate bond (O-H)in order to adhere to the TiO2 surface at an acidic pH. However, it was observed that modification of the structure of catechol upon oxidation at an elevated pH caused an increased bidentate bonding with the Ti atoms (O-Ti), while the strength of the DOPA-controlled adhesive interaction (O-H)with the substrate decreased. They indicated that DOPA containing adhesives have the potential to be used as effective coating materials if the reduction- oxidation activity can be regulated. While an exhaustive explanation of the mechanism of DOPA mediated binding still eludes the scientific community, many researchers have put forth a combination of studies that can help us better understand these mechanisms [2] [55]. Low yield of the MAP from mussel [54] has led researchers to develop synthetic compounds that have the ability to mimic the adhesive capabilities of the naturally occurring proteins. Dopamine methacrylamide (DMA), is a synthetic derivative of dopamine, and has been used by researchers as a monomer that imparts intrinsic adhesive properties to a polymer adhesive. Enhanced reversible adhesion, Paul glass et *al.* Mussel-inspired load bearing metalpolymer glues [46]. While most of the currently researched natural adhesive biomaterials like fibrin, collagen and gelatin based adhesives and a few synthetic glues like cyanoacrylate have poor wet adhesive property, polymer gels containing DMA present the possibility of a new sphere of bioadhesives that could help ameliorate the issue of poor adhesion in a wet environment that is posed by the

use of currently available natural and synthetic components.

AAPBA

Boronic acids have been widely used as chemical sensors that are capable of monitoring the blood sugar levels when they combine with glucose molecules. Based on their selective affinities for, they have also been used for the separation of carbohydrates and glycoproteins [51]. Also, Jun Yan et *al.* [30] suggested that the interaction between a boronic acid and a diol is probably the strongest reversible interaction among organic compounds that could occur in an aqueous medium. T The acrylamide functionality allows the relatively facile integration of the PBA into the HEAA network. The incorporation of AAPBA into the polymer network provides a simple means of preserving the adhesive utility of the catechol groups by formation of a catechol-boronic acid complex at basic pH and allows for the synthesis of a robust, pH sensitive hydrogel adhesive system. The adhesive utility of the catechol would be hampered without the presence of these protecting PBA groups. While being present in the hydrogel network, the contact mechanics tests have also demonstrated adhesive interaction of PBA groups with the borosilicate glass surface. DMA containing hydrogels have been proven to adhere to inorganic substrates under mildly acidic conditions [8]. However, the oxidation of catechol in a basic environment causes the adhesive properties to reduce significantly [17]. The specific role of the AAPBA in our work is that we propose that formation of reversible links between the boronic acid and the

catechol groups would render the hydrogel adhesive to not only be controlled upon command, but also increase its utility as it will theoretically be possible to use the same adhesive multiple times.

DMSO Polar aprotic solvent Although the major component of the hydrogel precursor is water, the synthetically derived DMA is insoluble in it. DMSO is hence used as a polar aprotic solvent to dissolve the DMA, AAPBA and is also soluble in water.

DI water Majority of the formulation is water, greater than 50

The borosilicate glass surface Capitol Brand M3504-1F Microscope slides 80% SiO2 , 13% B2O3 , 4% Na2O , 2-3% Al2O3 It provides a polar surface and is ideal to study the interactions between the hydrophilic hydroxyl and amino proteins in the DMA. Borosilicate glass is used in the manufacture of cooking utensils and lab apparatus. Critical products used as medical implants and devices used in space voyages are made of borosilicate glass and its derivatives. Borosilicate is widely used in implantable medical devices such as artificial eyes, synthetic hip joints, bone cements, and dental composite materials [56].

Encapsulating smaller and smarter implantables by GLASS ACTFRDRIC MAURON, (Former) SVP and Director of Active Implant Development for Valtronic Technologies Charbonnires, Switzerland; www.valtronic.com, Medical Design

As implantable biomedical sensors become smaller in size because of the advances in circuitry and metals like Titanium involved in the process of micro fabrication, the encapsulation of these fragile circuits is a new challenge faced by scientists. Most elements currently used for encapsulation have to be welded at high temperatures which eventually translates into comparatively bigger cases for shielding the circuit in a way that the circuit is not damaged in the process. The author mentions that the advantage in the case of glass is that it can be welded at relatively lower temperatures (800C) as opposed to laser- assisted metal welds. This process of welding requires a special enclosure and a controlled environment which can prove to be expensive. Although the author mentions that the absence of any adhesive is beneficial in terms of biocompatibility etc., our model hydrogel adhesive system is composed of biomaterials that have been proven to be biocompatible and are a part of many formulations. It expected that such inventions could be used in implants to aid hearing, and other sensors that could be implanted to gauge vital physiological parameters amongst other applications. In [56], the authors used borosilicate glass powder as the major veneering material for dental implants in order to impart good thermal expansion capabilities to the implant material. Borosilicate glass powder was also used as the coating material to provide thermal insulation via means of coated tiles in space shuttle orbiters ($HTTP://science.ksc.nasa.gov/shuttle/technology/sts-newsref/sts_sys.html$)

In order to demonstrate their adhesion studies using AFM , [47] used a smooth hemispherical glass surface to evaluate the repeatable adhesion capabilities of their

patterned microfibrillar structures under wet conditions. Hoyong Chung and Lee et *al.* [41] have stated that catecholic mediated adhesion can be facilitated by a coordination bond with an oxide surface. Yamamoto et *al.* [52] have indicated that the adhesive property of catechol containing adhesives is a combined effect of hydrophilic and hydrophobic interactions between the hydrophilic side chains that can form effective hydrogen bonds with a hydrophilic surface like glass. When polymer adhesives containing mussel adhesive protein were tested against a high surface energy glass surface, the hydrophilic pendant catecholic groups interacted with the highly hydrophilic glass surface to form strong adhesive bonds in a wet environment.

Why hemispherical hydrogel?

Paul Glass et *al.*[47] suggests that it eliminates misalignment problems during testing and provides a surface with well defined roughness

Appendix B

Compilation of images

B.1 Additional information for polymer structures

B.2 Contact mechanics images

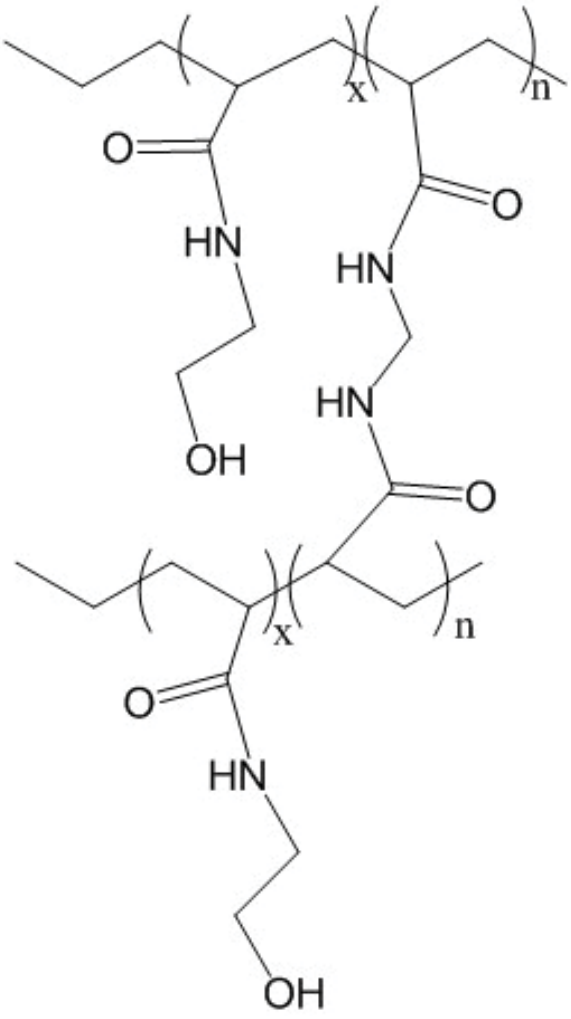

Figure B.1: HEAA+MBAA

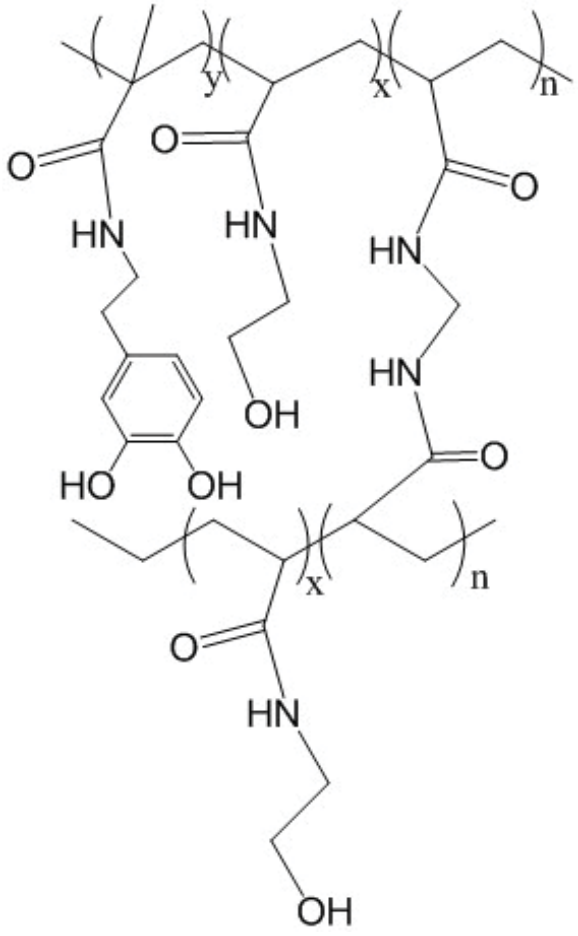

Figure B.2: HEAA+MBAA+DMA

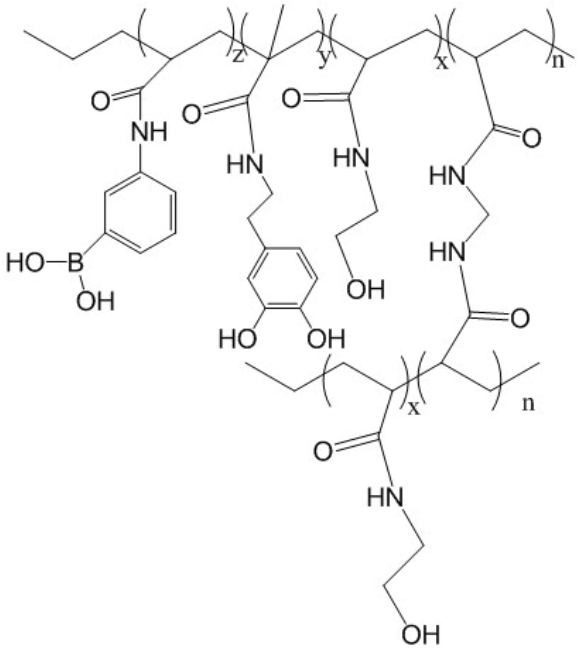

Figure B.3: HEAA+MBAA+DMA+AAPBA

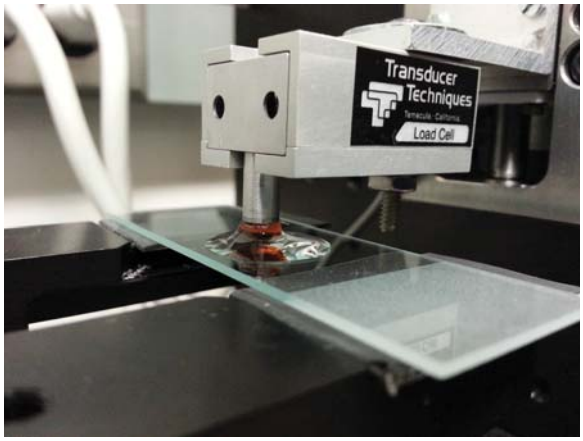

Figure B.4: Actual representation of the stem from the contact mechanics test in which the equilibrating procedure of the hemispherical hydrogel adhesive with $250\mu m$ of the pH 9 buffer solution

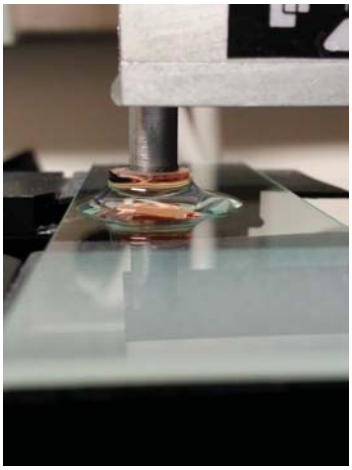

Figure B.5: Actual representation of the stem from the contact mechanics test in which the equilibrating procedure of the hemispherical hydrogel adhesive with $250\mu m$ of the pH 9 buffer solution

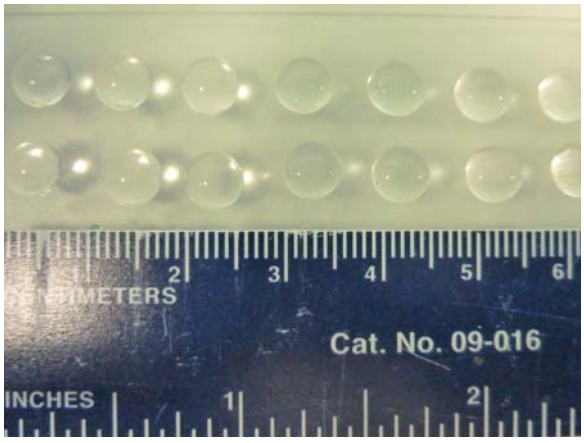

Figure B.6: An image showing the synthesized hemispherical hydrogels

B.3 Images of the hydrogel discs

Figure B.7: An image showing the synthesized hydrogel discs: Right after synthesis, the 2 mm-thick hydrogel sheets were cut into 15 mm discs, following which they were equilibrated in acidic and basic pH buffered solutions

B.4 Additional information for rheological analyses

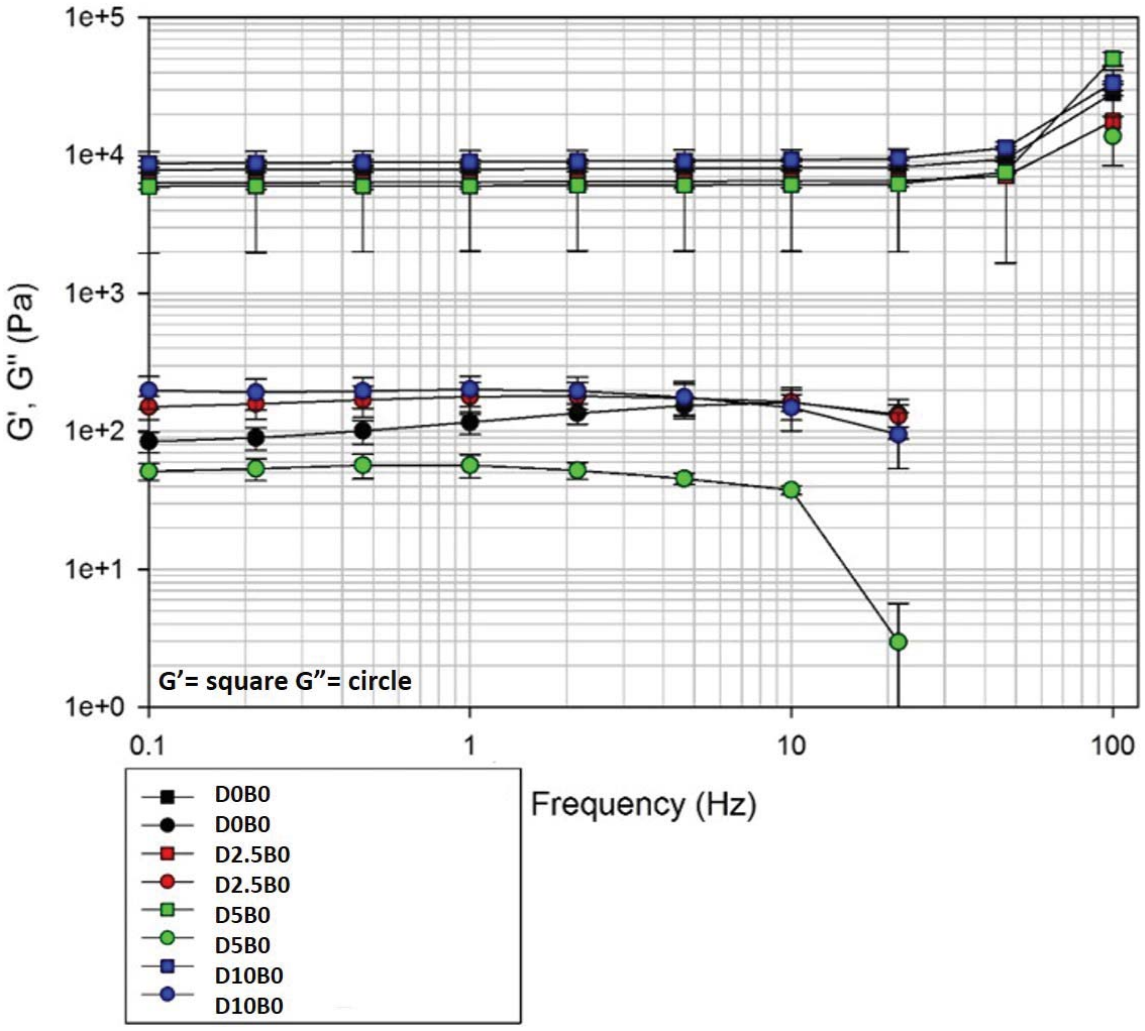

Figure B.8: Comparing the storage and loss moduli for increasing amounts of DMA at pH 3

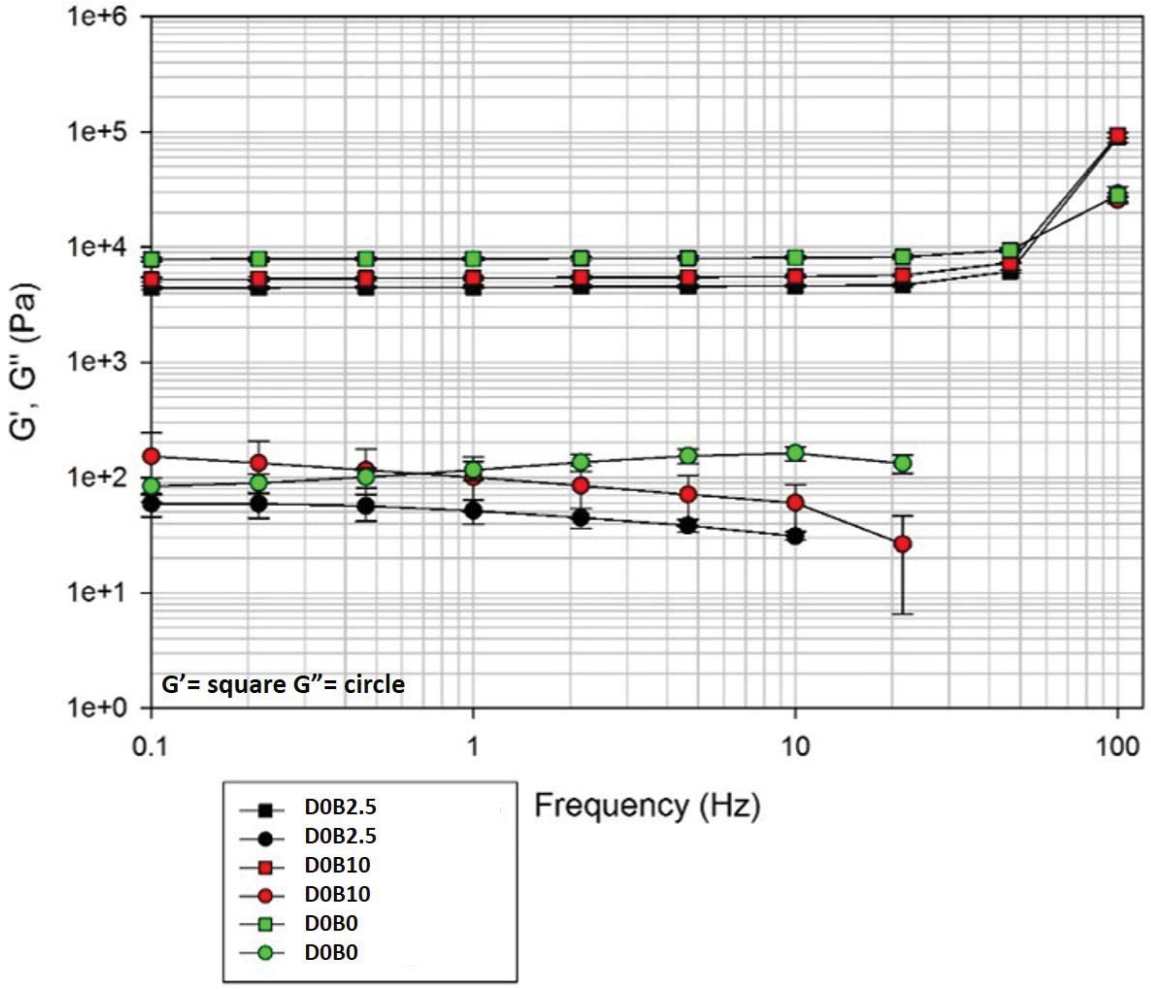

Figure B.9: Comparing the storage and loss moduli for increasing amounts of AAPBA at pH 3

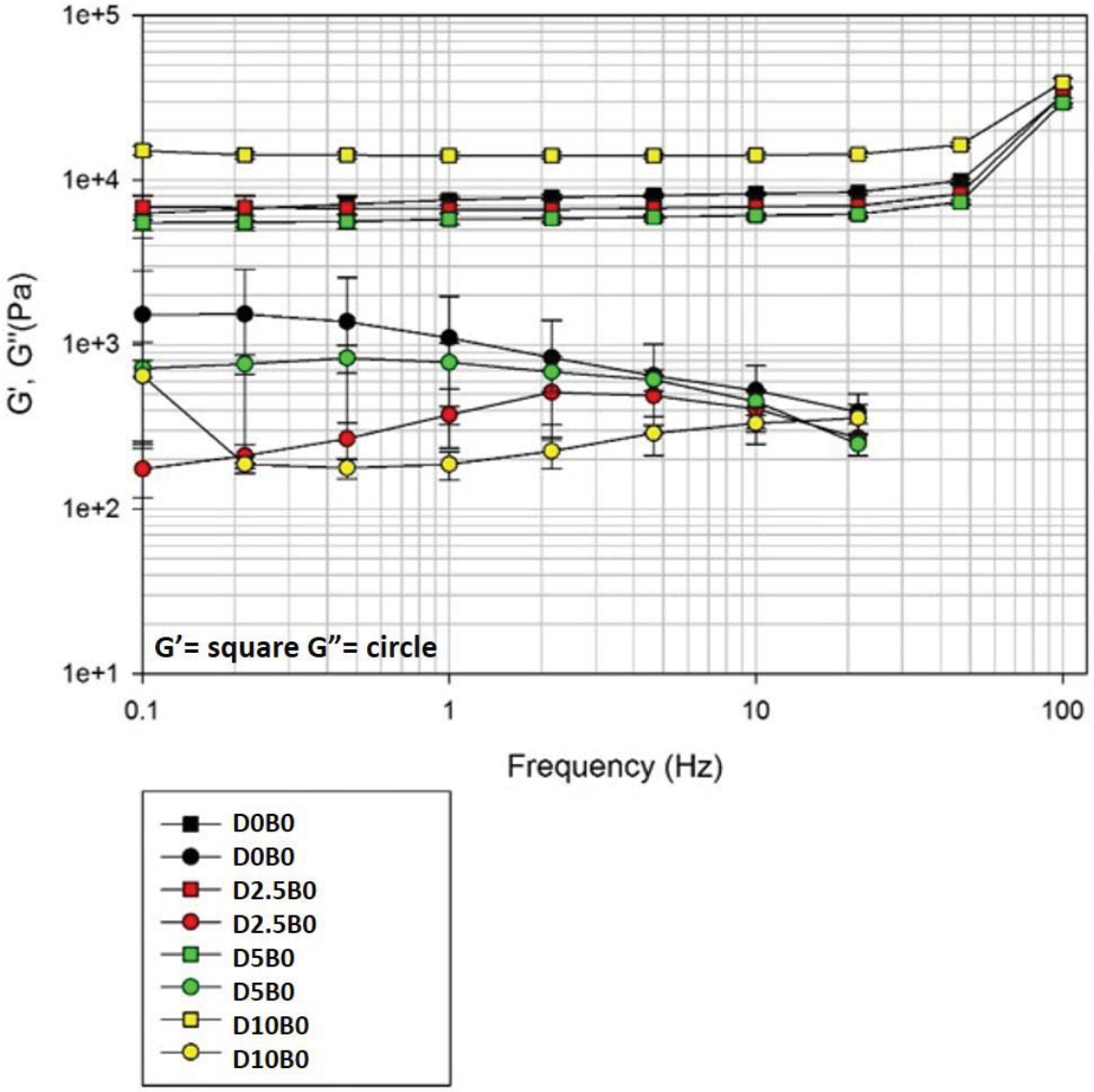

Figure B.10: Comparing the storage and loss moduli for increasing amounts of DMA at pH 9

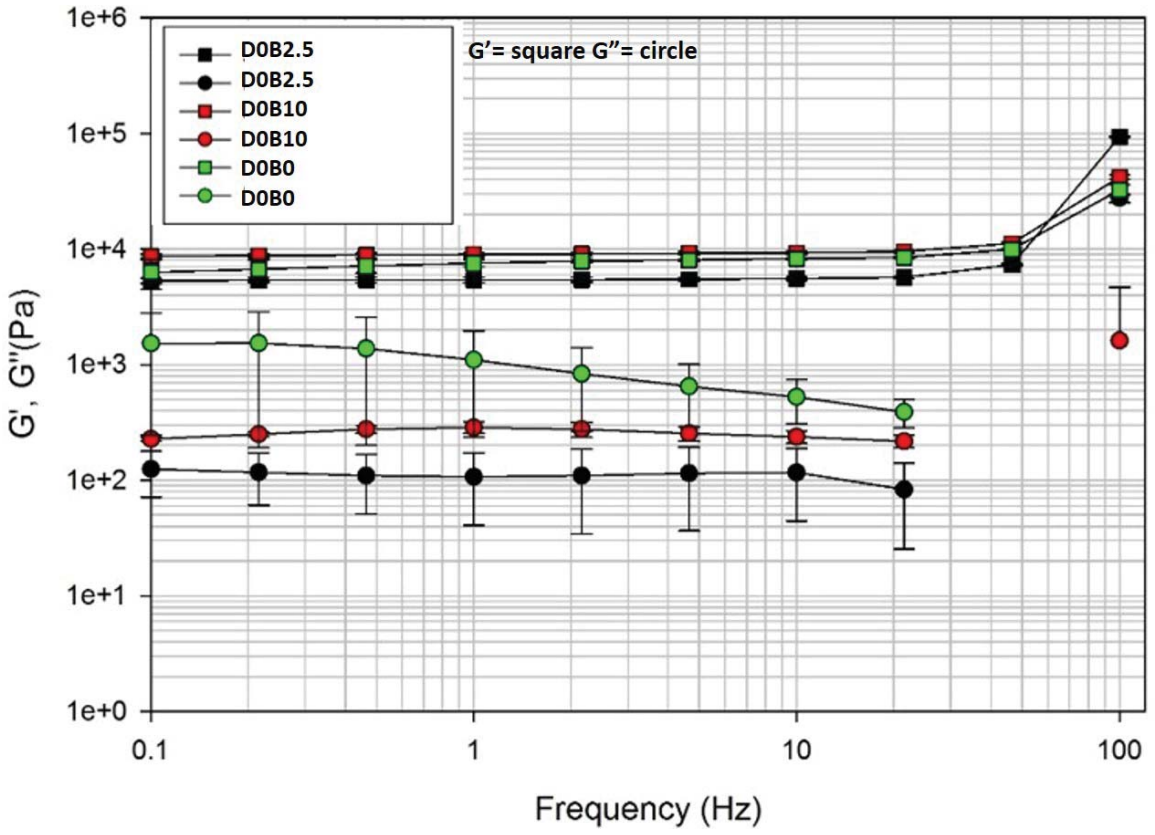

Figure B.11: Comparing the storage and loss moduli for increasing amounts of AAPBA at pH 9

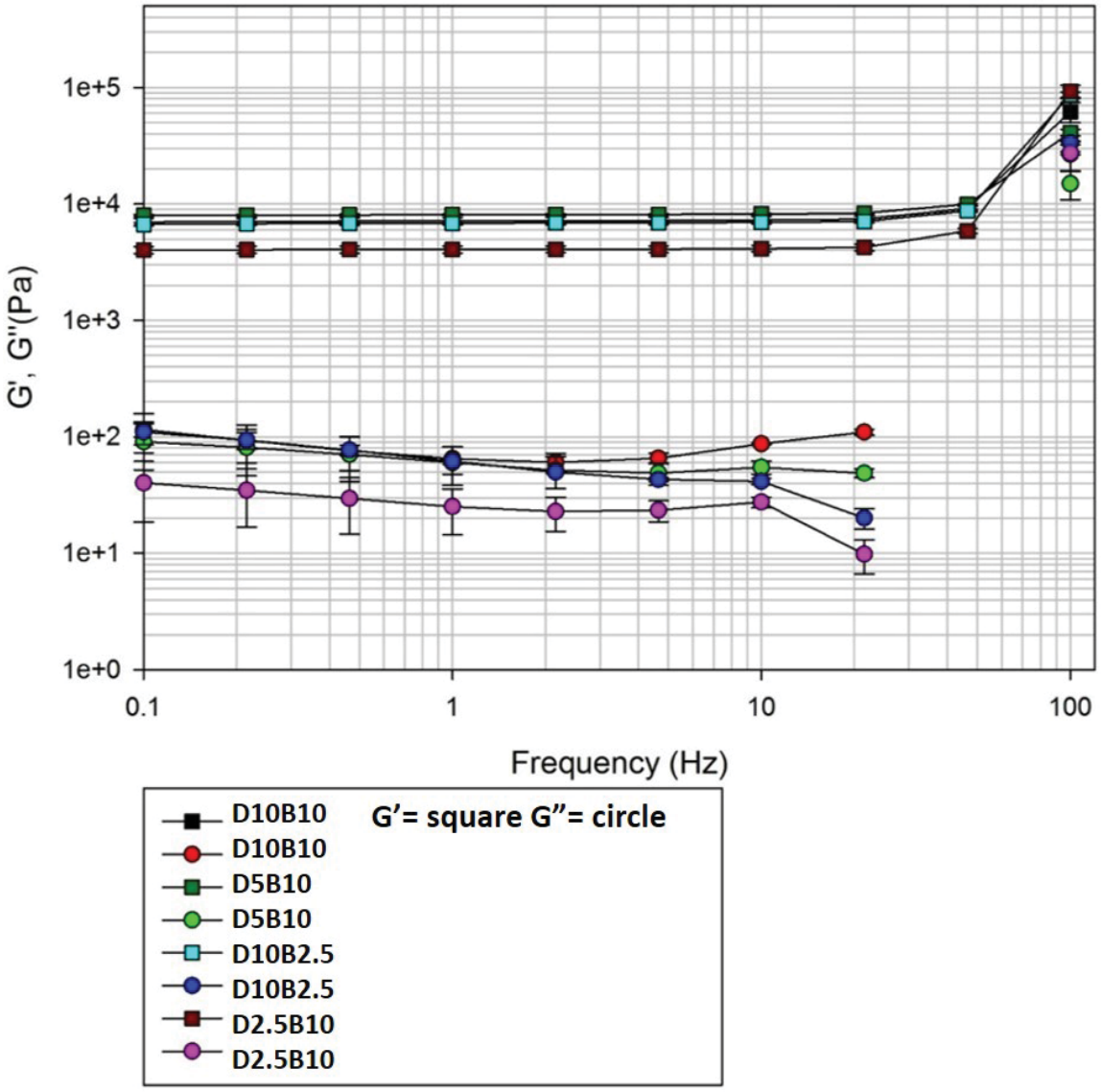

Figure B.12: Comparing the storage and loss moduli for varying compositions of DMA and AAPBA at pH 3

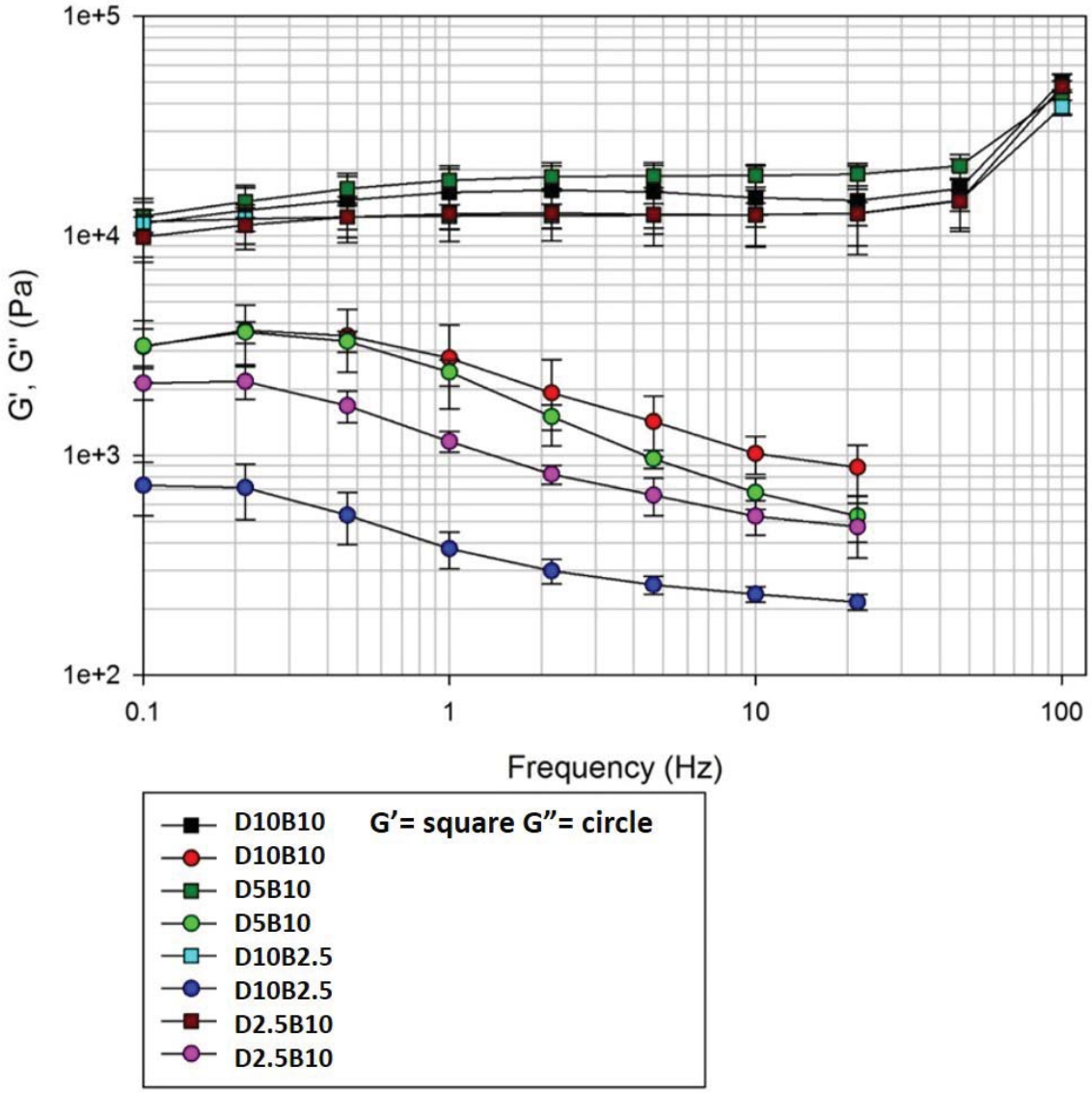

Figure B.13: Comparing the storage and loss moduli for varying compositions of DMA and AAPBA at pH 9

Appendix C

Letters of Permission

This is a License Agreement between Ameya R Narkar ("You") and Nature Publishing Group ("Nature Publishing Group"). The license consists of your order details, the terms and conditions provided by Nature Publishing Group, and the payment terms and conditions.

All payments must be made in full to CCC. For payment instructions, please see information listed at the bottom of this form.

License Number 3687691464755

License date Aug 14, 2015

Licensed content publisher Nature Publishing Group Licensed content publication Nature Communications

Licensed content title Impact tolerance in mussel thread networks by heterogeneous material distribution

Licensed content author Zhao Qin, Markus J. Buehler

Licensed content date Jul 23, 2013 Volume number 4 Type of Use reuse in a dissertation / thesis

Requestor type academic/educational

Format print and electronic

Portion figures/tables/illustrations Number of figures/tables/illustrations 1

Highres required no

Figures 1(a)

Author of this NPG article no

Your reference number None Title of your thesis / dissertation pH Responsive, Adhesive Hydrogels based on Reversible Catechol-Boronic Acid Complexation

Expected completion date Aug 2015

Estimated size (number of pages) 100

Total 0.00 USD